URINARY VOLATILE ORGANIC COMPOUNDS FOR DETECTION OF BREAST CANCER AND MONITORING CHEMICAL AND MECHANICAL CANCER TREATMENTS IN MICE

A Thesis

Submitted to the Faculty

of

Purdue University

by

Meghana Teli

In Partial Fulfillment of the

Requirements for the Degree

of

Master of Science in Biomedical Engineering

May 2019

Purdue University

Indianapolis, Indiana

THE PURDUE UNIVERSITY GRADUATE SCHOOL
STATEMENT OF THESIS APPROVAL

Dr. Hiroki Yokota, Co-Chair

Department of Biomedical Engineering

Dr. Mangilal Agarwal, Co-Chair

Department of Mechanical Engineering

Dr. Julie Ji

Department of Biomedical Engineering

Approved by:

Dr. Julie Ji

Head of the Graduate Program

I dedicate this work to my family, my pillars of strength and thank them for their endless backing, love and care.

ACKNOWLEDGMENTS

I want to express my special thanks of gratitude to my advisors, Dr. Hiroki Yokota and Dr. Mangilal Agarwal for giving me the opportunity to work on their collaborative project. I offer my sincere appreciation for their immense support, mentorship and encouragement during the two years of my thesis work. I also thank my committee member, Dr. Julie Ji for her suggestions and encouragement.

To obtain the results described in this thesis, I analyzed urine specimens on gas chromatography-mass spectrometry, conducted data preprocessing (including data normalization treatments) followed by univariate and multivariate analyses to identify features of interest. I further identified compounds using mass spectral data and sequentially completed metabolic pathway analysis of identified compounds. I would like to acknowledge the colleagues and collaborators who worked with me.

I would like to thank Integrated Nanosystems Development Institute and its members. The patience, persistent help and motivation provided by Dr. Amanda Siegel is heartening. I thank her for her guidance and inputs in learning new analysis techniques which I was able to develop for my project. I take this opportunity to acknowledge the selfless support of Mark Woollam, who led the way in optimization of parameters for gas chromatography of urine headspace. I am grateful to Dr. Ali Daneshkhah for the Matlab algorithms he wrote, and teaching me how to use them and adapt them for my studies. As mouse urine analysis was an ancillary study, I assisted members of Dr. Yokota's lab in mouse urine collection. I admire the efforts of Andy Chen, Dr. Shengzhi Liu, Luqi Wang, Yao Fan, Yue Wang and Aydin Jalali for their work in conducting animal modeling experiments. Lastly, I thank Paula Angarita, Paul Grocki, Sanskar Thakur, and Dan Minner.

Special mention for the constant assistance given by Sherry Clemens with the administrative work has made my boat of graduate studies sail smooth.

TABLE OF CONTENTS

Page

LIST OF TABLES

LIST OF FIGURES

Figure Page

LIST OF ABBREVIATIONS

VOCs	Volatile Organic Compounds
SPME	Solid Phase Micro Extraction
GCMS	Gas Chromatography Mass Spectrometry
QTOF	Quadrupole Time of Flight
VIF	Variation Inflation Factor
PCA	Principal Component Analysis
LDA	Linear Discriminant Analysis
LOOCV	Leave One Out Cross Validation
TFP	Trifluoperazine
FP	Fluphenazine
HER	Human Epidermal Growth Factor Receptor
ECM	Extra Cellular Matrix
OPN	Osteopontin
PTHrP	Parathyroid hormone-related peptide
IL	Interleukin
IGF	Insulin-like Growth Factor
PDGF	Platelet Derived Growth Factor
TGF	Transforming Growth Factor
CA	Cancer Antigen
CEA	Carcinoembryonic Antigen

ABSTRACT

Teli, Meghana M.S.B.M.E., Purdue University, May 2019. Urinary Volatile Organic Compounds for Detection of Breast Cancer and Monitoring Chemical and Mechanical Cancer Treatments in Mice. Major Professors: Hiroki Yokota, Mangilal Agarwal.

The aim of this study is to identify metabolic transformations in breast cancer through urinary volatile organic compounds in mammary pad or bone tumor mice models. Subsequently, it focuses on investigating the efficacy of therapeutic intervention through identified potential biomarkers. Methods for monitoring tumor development and treatment responses have technologically advanced over the years leading to significant increase in percent survival rates. Although these modalities are reliable, it would be beneficial to observe disease progression from a new perspective to gain greater understanding of cancer pathogenesis. Analysis of cellular energetics affected by cancer using bio fluids can non-invasively help in prognosis and selection of treatment regimens. The hypothesis is altered profiles of urinary volatile metabolites is directly related to disrupted metabolic pathways. Additionally, effectiveness of treatments can be indicated through changes in concentration of metabolites. In this ancillary experiment, mouse urine specimens were analyzed using gas chromatography-mass spectrometry, an analytical chemistry tool in identifying volatile organic compounds. Female BALB/c mice were injected with 4T1.2 murine breast tumor cells in the mammary fat pad. Consecutively, 4T1.2 cells were injected in the right iliac artery of BALB/c mice and E0771 tumor cells injected in the tibia of C57BL/6 mice to model bone tumor. The effect of two different modes of treatment: chemical drug and mechanical stimulation was investigated through changes in compound profiles. Chemical drug therapy was conducted with dopamine agents, Trifluoperazine, Fluphenazine and a statin, Pitavastatin. Mechanical stimulation in-

cluded tibia and knee loading at the site of tumor cell injection were given to mice. A biological treatment mode included administeration of A5 osteocyte cell line. A set of potential volatile organic compounds biomarkers differentiating mammary pad or bone confined tumors from healthy controls was identified using forward feature selection. Effect of treatments was demonstrated through hierarchical heat maps and multivariate data analysis. Compounds identified in series of experiments belonged to the class of terpenoids, precursors of cholesterol molecules. Terpene synthesis is a descending step of mevalonate pathway suggesting its potential role in cancer pathogenesis. This thesis demonstrates the ability of urine volatilomics to indicate signaling pathways inflicted in tumors. It proposes a concept of using urine to detect tumor developments at two distinct locations as well as to monitor treatment efficacy.

1. INTRODUCTION

Breast cancer in women is estimated to account for thirty percent of new cancer cases in the United States in 2019 (Figure 1.1) [1]. Lifestyle choices, reproductive factors and environment are few of the underlying causes of breast cancer morbidity and mortality [2]. Risk factors generally belong to two classes: (a) modifiable risk elements including obesity, consumption of alcohol, smoking and (b) fixed elements such as age and genetics [3].

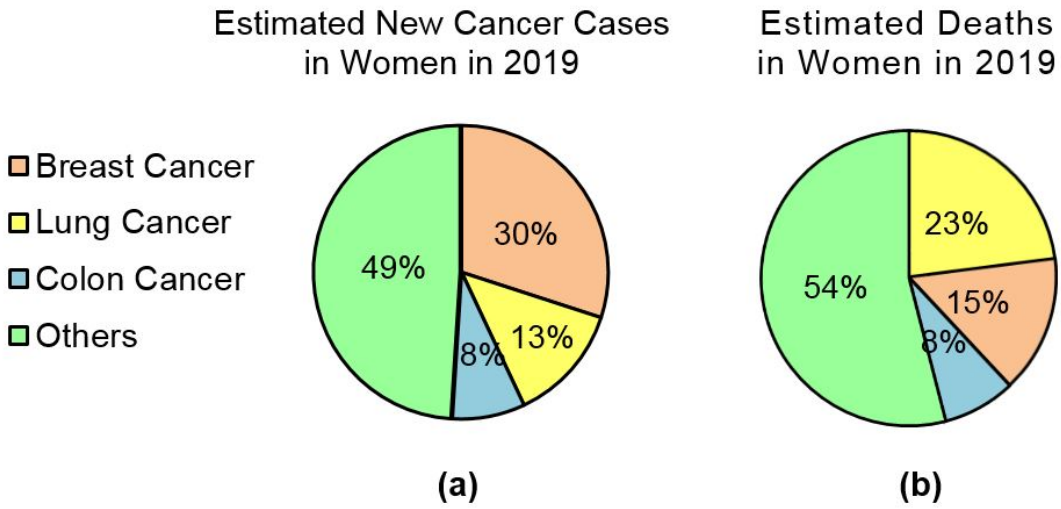

Fig. 1.1.: (a)Breast cancer accounting for 30% of total estimated new cancer cases diagnosed in women in 2019, (b) Breast cancer associated deaths accounting for 23% of total estimated cancer deaths in women in 2019 (US based results). [1]

Various systems used for breast cancer classification are based on stage, receptor status, grade, histopathology and DNA assays among others [4]. Cancers developing from ducts and lobules are ductal and lobular carcinomas, respectively [5]. Tumors initially formed in the inner lining of ducts or lobules, classified as carcinoma in

situ gradually invade surrounding tissues and develop distant metastases (Figure 1.2. A) [6]. Presence of receptors for hormones, estrogen, progesterone, HER2, are also responsible for cancer cell proliferation and migration (Figure 1.2. B) [7]. Grading of breast tissue into well differentiated (low grade), moderately differentiated (intermediate grade), and poorly differentiated (high grade) is described by the overall appearance of the cancer cells (Figure 1.2. C) [8]. The complex inter-relationship of these characteristics govern prognosis and treatment response.

1.1 Breast Cancer and Metastasis

The distant relapse of secondary metastases due to cancer cell extravasation from primary tumor site is the leading reason of breast cancer-associated deaths [9]. Figure 1.2. A illustrates the metastatic cascade in breast cancer starting with cells intruding local surrounding tissues and eventually disseminating to other organs through bodys circulatory system [6]. Initially, continuous cell division and growth within the primary tumor leads to invasion of the tumor border and intravasation of the circulatory system. The potential of a tumor cell to metastasize is explained by the seed and soil hypothesis [10] with cell extravasation and formation of micro metastases inside a secondary site. The process is assisted by epithelial-mesenchymal transition that involves degradation of ECM for cell migration [9]. Metastatic breast cancer are generally diagnosed several years after the incidence of primary tumors, however, they are rarely diagnosed before clinical diagnosis of primary breast cancers [11]. Tumors have a tendency to undergo organ-specific metastasis [12]. In breast cancer, the common location of secondary tumor growth is in brain, bone, lungs, liver with bone and lungs being frequent of all (Figure 1.3. A) [13]. The patterns observed in selection of organs are associated with a plethora of micro-environmental, cellular and molecular factors [14].

For breast cancer associated bone metastasis, luminal cancer subtypes have a higher development rate (80%) than basal-like (41.7%) and HER2-like tumors (55.6%).

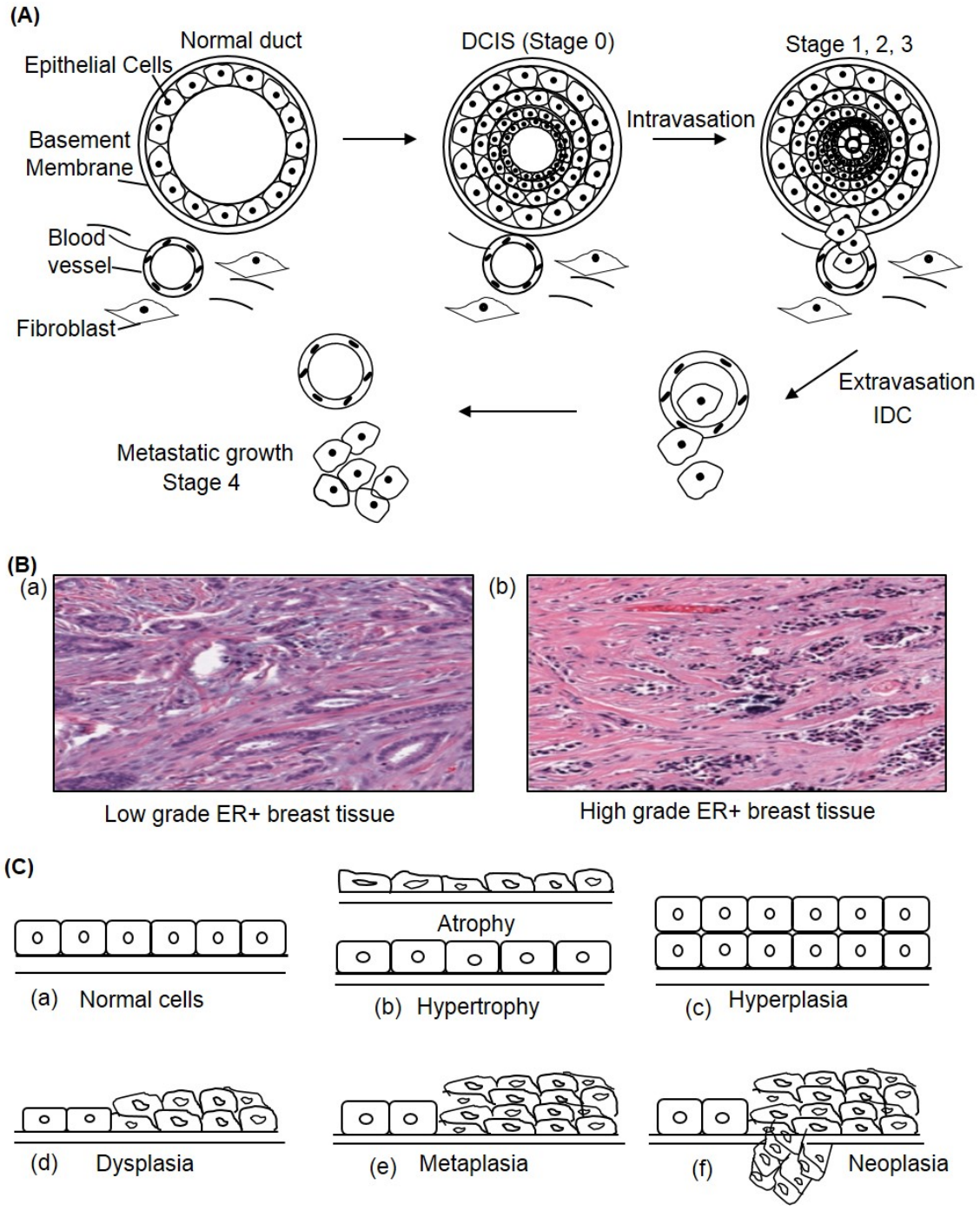

Fig. 1.2.: Classification of breast cancer based on (A) Stages (1-4) corresponding to the degree of tumor cells spreading from within duct (Ductal Carcinoma In Situ (DCIS)) to lymph nodes (Invasive Ductal Carcinoma (IDC)) and other body parts (B) Histopathology [8] and (C) Grade corresponding to cell differentiation.

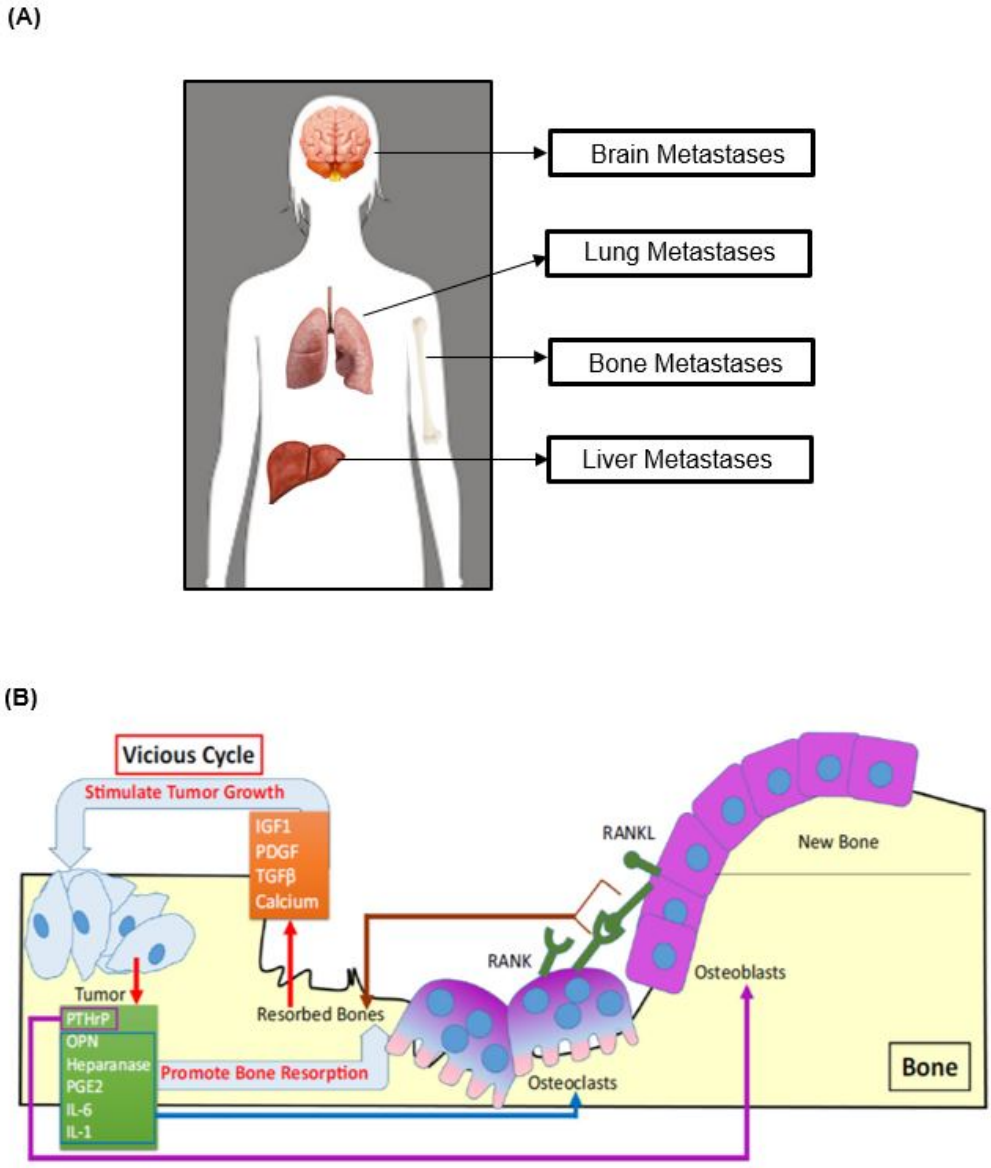

Fig. 1.3.: Breast Cancer and Metastasis (A) Brain, lung, bone and liver are the common locations for breast cancer metastasis.(B) Breast cancer metastasis to bone. Enhanced bone resorption by tumor-derived factors, OPN, PTHrP, heparanase, IL-1. Tumor growth stimualtors, IGF1, PDGF, TGF, and calcium secreted by resorbed bone. [15]

Figure 1.3. B is a schematic of growth mediated metastatic tumor proliferation in bone showing elevated bone resorption. Tumor-derived factors such as osteopontin (OPN), parathyroid hormone-related peptide (PTHrP), heparanase, IL-6 enhance bone resorption. Next, the resorbed bone releases IGF1, PDGF, TGF- and calcium essential for tumor proliferation. The cycle of bone resorption and tumor growth is analogous to the seed and soil hypothesis of organ specific metastasis with elements secreted in the microenvironment making the soil fertile for tumor cells (seeds) to survive. Similarly, up-regulation of RANKL activates osteoclast differentiation and ultimately adds to bone resorption [15].

In this study, two murine cancer cell lines, 4T1.2 and E0771 were utilized to induce tumor in mammary pad or bone. 4T1.2 cell line is a clone of 4T1 cells used as a stage IV human breast cancer equivalent for animal modelling experiments. E0771 is a spontaneously developing breast adenocarcinoma cell line.

1.2 Breast Cancer Diagnosis

The initial step in diagnosing breast cancer is screening or identifying symptoms that finally prompt to diagnostic procedures (Figure 1.4) [16]. Screening is generally associated with smaller tumors with lower probability of metastasis and better treatment response and progression free survival [16]. One of the common screening methods is mammography which is responsible to lower mortality rates by 19% [17]. However, some of the negative aspects of its application are: it induces anxiety and negative psychological effects and also has a potential risk of exposure to radiation (increases chances of cancer pathogenesis). Another way of inspection is through physical examination of the breast skin [18]. It is performed by palpation of the breast parenchyma to ascertain size, mobility and number of lymph node basins. The outcomes of this technique are not reliable and therefore utilization of other modalities is necessary to validate diagnosis. Other imaging techniques, MRI and CT also have limited use in clinical systems due to high operational and maintenance costs [19, 20].

Second, while ultrasound is cost effective these tests usually fail to detect ductal or lobular tumors. The inability of CT to distinguish tissues with abnormal properties as a tumor or scar tissue also makes it an inaccurate tool [21].

A definitive method of breast cancer diagnosis is through examination of breast tissue. There are several biopsies adopted to account for limitations with the screening procedures discussed earlier. These include core biopsy, excision biopsy and fine needle aspiration [16]. Typically, a piece of tissue or cell sample is obtained from the subject and analyzed in a laboratory. These tests although give comprehensive pathologic results and differentiate benign and malignant tumors; a critical risk of their use involves breaking the skin barrier that can potentially help in developing infection or bleeding.

Molecular based methods for monitoring tumor development include analysis of DNA [22], RNA [23], proteins [24, 25], volatile organic compounds (VOCs) and other metabolites [26]. Blood based assays to identify predictive tumor markers are innovative procedures for early detection of cancer. Serum based biomarkers, CA 15-3, CEA, CA 27-29 are analyzed but have false discovery rates due to low sensitivity and specificity [27]. Complete blood count of various cell types, blood protein testing are examples of bio fluid based cancer diagnosis approach [28].

1.3 Breast Cancer Treatment and Monitoring

The conventional treatment procedures cover a combination of local and systemic therapies for breast cancer (Figure 1.5). The endpoint of treatment in non-metastatic tumors from breast and regional lymph nodes while cancer is in its primitive stage. In case of metastasis, the goal is of progression free survival and to safeguard surrounding tissues from tumor cells. Surgical resection and radiation are ways of therapeutic intervention with tumor development locally [29]. Usually, breast conserving and non-breast conserving approaches are adopted depending on the extent of tumor progression. The former involves surgical incision on the breast for removal of tumor

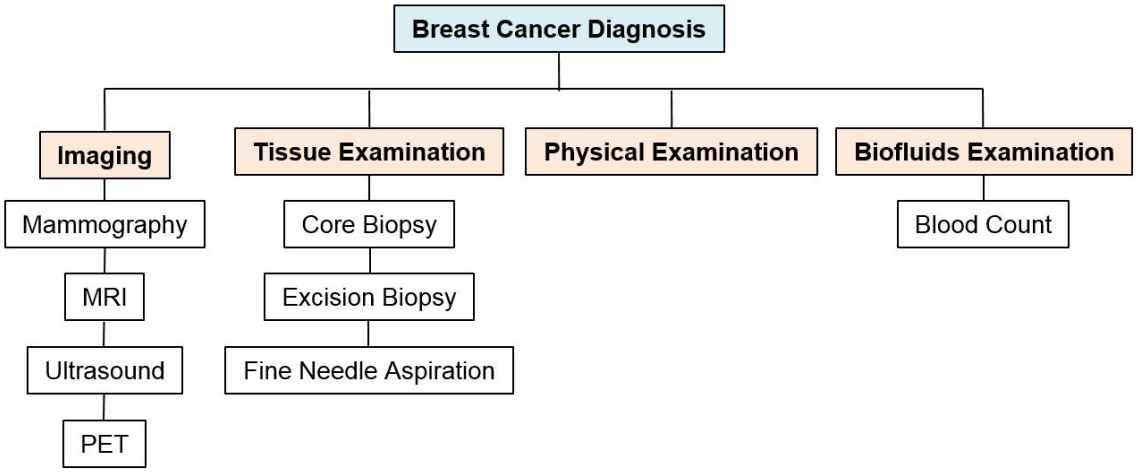

Fig. 1.4.: Major classes of breast cancer diagnostic approaches including imaging techniques, tissue examination through biopsies, physical examination for breast lump or fluid discharge and bio fluids examination for analysis of circulating tumor cells or protein, DNA, RNA biomarkers. [17–21]

while maintaining total tissue planes [16]. Non-breast conservation method is the complete removal of the diseased breast in women having extensive calcification or develop side effects to radiation therapy [16]. Additionally, reports suggest the synergistic effect of breast conserving approaches with radiation have a comparable overall survival rates in patients treated with non-conserving approaches.

Systemic procedures include chemotherapy [30], hormone therapy [31] and targeted therapy where therapeutic agents are administered intravenously or given to the patients through oral drugs. The timeline for chemotherapies range between three to six months or even few weeks [21]. Neoadjuvant treatment is shrinkage of tumor through medicines given to patients prior to conducting surgical procedures [32]. Furthermore, adjuvant treatment refers to prescription of drugs after surgical removal of tumor to prevent recurrence of disease. Controlling actions of hormones, estrogen and progesterone towards tumor proliferation is the essence of hormonal therapy. This mode is usually adapted before surgery to decrease tumor size and increase

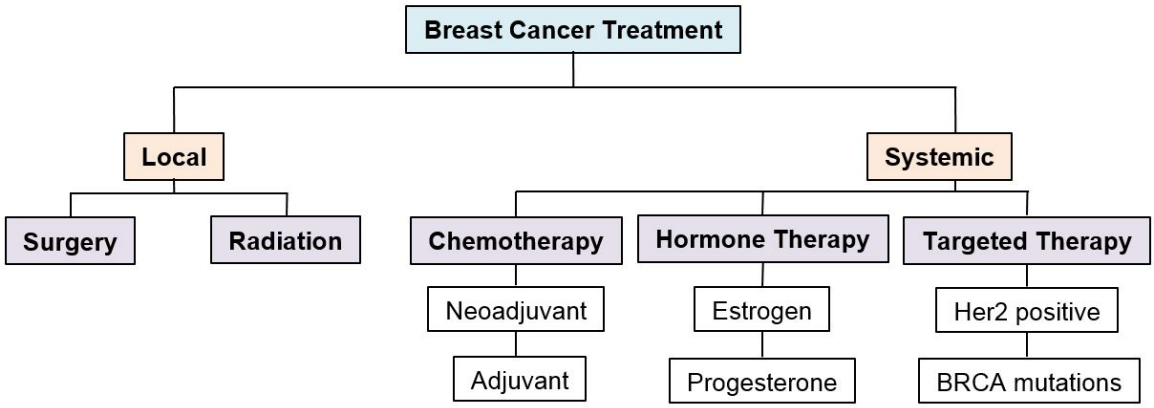

Fig. 1.5.: Major classes of breast cancer treatment procedures including local and systemic approaches. Local modalities are directed to the affected area while systemic modalities are administered intravenously or orally. [16, 21, 29–31]

options for treatment. Targeted therapies are directed towards molecular agents or pathways crucial in the development of cancer. Some of agents of targeted therapies include capecitabine [33], a drug for metastatic breast cancer; tyrosine-kinase inhibitors; PARP inhibitors; androgen receptor inhibitors. Diagnostic tests are also used for tracking therapeutic responses and corresponding tumor growth [36]. The frequency of monitoring depends on the clinical stage, toxicity of therapy and auxiliary factors [18]. One of the common ways of assessing tumor size is through physical examination of the affected area but these often result in incorrect prognosis. Moreover, imaging methods such as PET, MRI, x-ray and CT are expensive [20, 21] and frequent use of these pose a potential harm of exposure to radiation [20]. Lastly, due to delayed effect (6-8 weeks) on tumor size with chemotherapy, [19] if the treatment is not efficient, it will be detected after the patient has received harmful radiation for a prolonged period of time.

A non-invasive technique to monitor treatment efficacy would decrease over treatment in patients and aid in the decision-making process. Although contemporary procedures have been in clinical use for decades, conceptualization and development

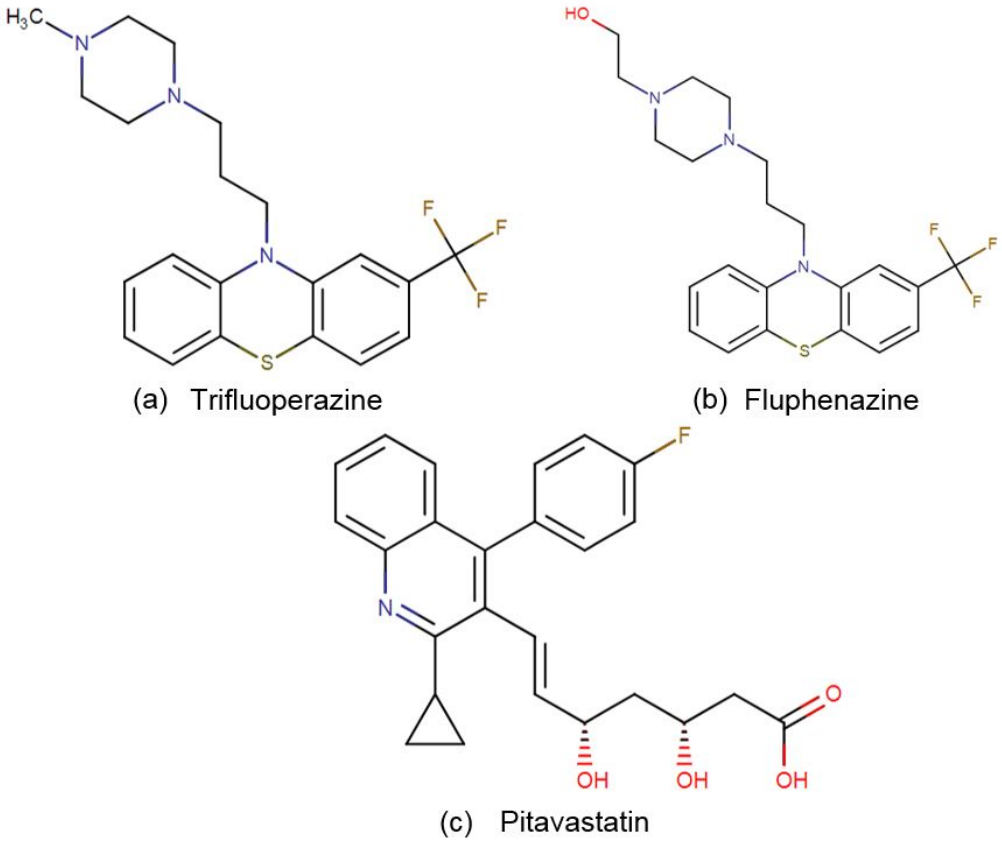

Fig. 1.6.: Chemical treatment of mammary pad or bone tumors through (A) Trifluoperazine,a phenothiazine is used as an antipsychotic and an antiemetic, (B) Fluphenazine, a phenothiazine used in the treatment of psychoses, Both the drugs block the postsynaptic mesolimbic dopaminergic D1 and D2 receptors in the brain and depress reticular activating system thus affecting basal metabolism, body temperature, wakefulness, vasomotor tone, and emesis (C) Pitavastatin, belongs to the family of statins and lowers lipid concentration by inhibiting mevalonate pathway. It is used for primary and secondary prevention of cardiovascular disease. [34, 35]

of an alternative, non-invasive biological assay would give insights into factors that contribute to tumor development. Recent studies involving blood analysis of circulating tumor DNA unveil a promising tool for determining treatment efficacy [37]. However, these studies are based on assumptions that mutations examined are entirely due to cancer and overlook the probability of clonal hematopoiesis [38]. Furthermore,

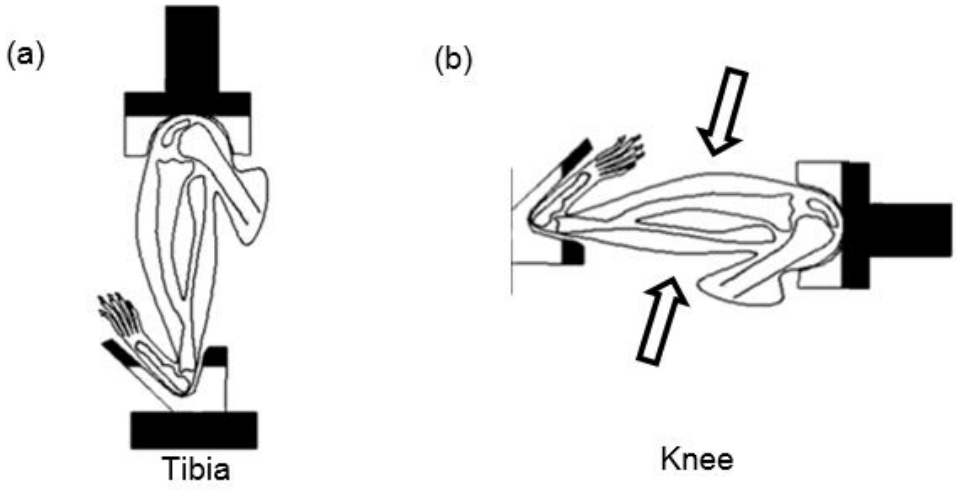

Fig. 1.7.: Mechanical treatment of mice (A) Tibia loading involves direct mechanical loading at the site of tumor cell injection, (b) Knee loading involves direct mechanical loading lateral to the site of tumor cell injection.

circulating tumor cell counts have failed to provide a predictive value in patients undergoing first-line chemotherapies [18].

For the purpose of this thesis, mice with tumors in mammary pad or bone were administered with three different drugs in three different studies to investigate their effect of tumor size reduction. Dopamine modulators, Trifluoperazine and Fluphenazine are used as antipsychotic medications and involved in neurological functions [34, 39, 40]. Pitavastatin is a statin inhibiting 3-hydroxy-3-methyl-glutaryl-CoA (HMG-CoA) reductase of cholesterol synthesis pathway [35]. Pre-clinical and clinical evidences show inhibitory action of statins on tumor. The mevalonate pathway is not only essential in cholesterol synthesis and lipid metabolism but also affects tumor progression [41, 42], and prenylation [43] vital for tumor growth . Another group of mice bearing bone tumor were treated by mechanical stimulation of tibia to understand the effect of physical activity on bone resorption and tumor size.

1.4 Breast Cancer and Metabolomics

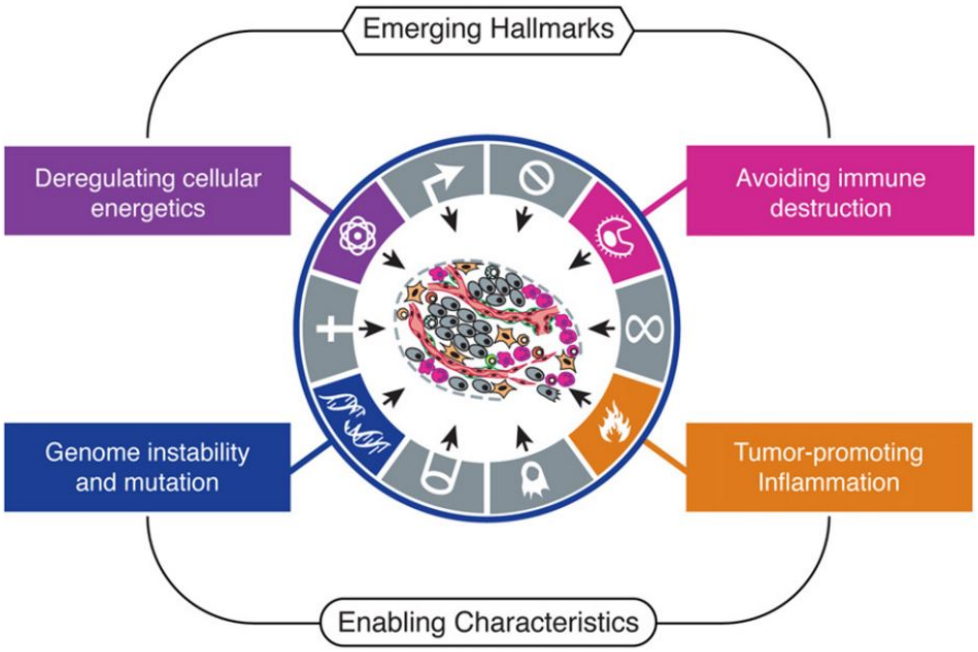

Fig. 1.8.: Emerging cancer hallmarks - Deregulating cellular energetics and avoiding immune destruction for transformation of normal cells to tumor cells. [44]

The heterogeneous nature of cancer has been demonstrated through several omics based platforms [45–49]. Tumor biology of breast cancer has been studied through various immuno-histochemical markers and gene expression profiling [50]. A recent advancement in the field of omics is the study of metabolites called metabolomics and volatilomics. One of the hallmarks of cancer is deregulation of cellular energetics (Figure 1.8.) affecting cellular proliferation, invasion and metastasis [44]. Therefore, in-depth understanding of cancer pathophysiology could be gained through analysis of metabolic changes related with cancer. Sequentially, this information can also help in developing novel targeted therapeutics. Moreover, the one model fits all strategy of traditional treatment options is deemed to be imperfect due to distinct tumor characteristics. The growing knowledge about complexities of breast cancer pathogenesis

demand tailoring personalized systemic and regional therapies to increase efficacy and decrease unnecessary morbidity [51]. Monitoring therapeutic effect can aid in patient decision-making throughout the course of treatment and potentially help clinicians advance personalized medicine.

A typical workflow of breast cancer metabolomics study is shown in Figure 1.9. First, a stimulation by incidence of cancer alters metabolic pathways [52]. Samples are collected from tissue, plasma, urine, breath and metabolites are analyzed by extraction using mass spectrometric or nuclear magnetic resonance techniques. Data acquisition and relevant data analysis procedures are used to identify biomarker signatures. Next, pathway analysis is conducted to correlate biomarkers with metabolic axes. For the purpose of this experiment, GCMS QTOF was used as a separation method to incubate and extract metabolites from samples through SPME and sequentially detect metabolites. Symbolically, distribution of metabolites is visualized using dimensionality reduction algorithms, PCA or LDA. Identified metabolites are eventually probed for their potential involvement in metabolic pathways.

1.4.1 Volatile Organic Compounds as Biomarkers

VOCs are intermediates or final products of metabolic pathways and can provide potential metabolic information about disease through their unique scent/odor [26]. In addition to changes in metabolism due to the tumor, microbial metabolism in the gut microflora also contributes towards production of VOCs [53]. VOC analysis is conducted non-invasively in urine, sweat, breath and other biological samples [54]. As these are fingerprints of the bodys metabolism, their investigation can provide an understanding of the changes occurring due to disease. Studies have proposed a signature of VOCs that have different concentrations in samples collected from diseased patients when compared to healthy controls. [55–60].

Potential biomarkers for breast cancer were previously reported from biological breath samples (Figure 1.10.) [61–64]. One of the studies identified a set of VOCs

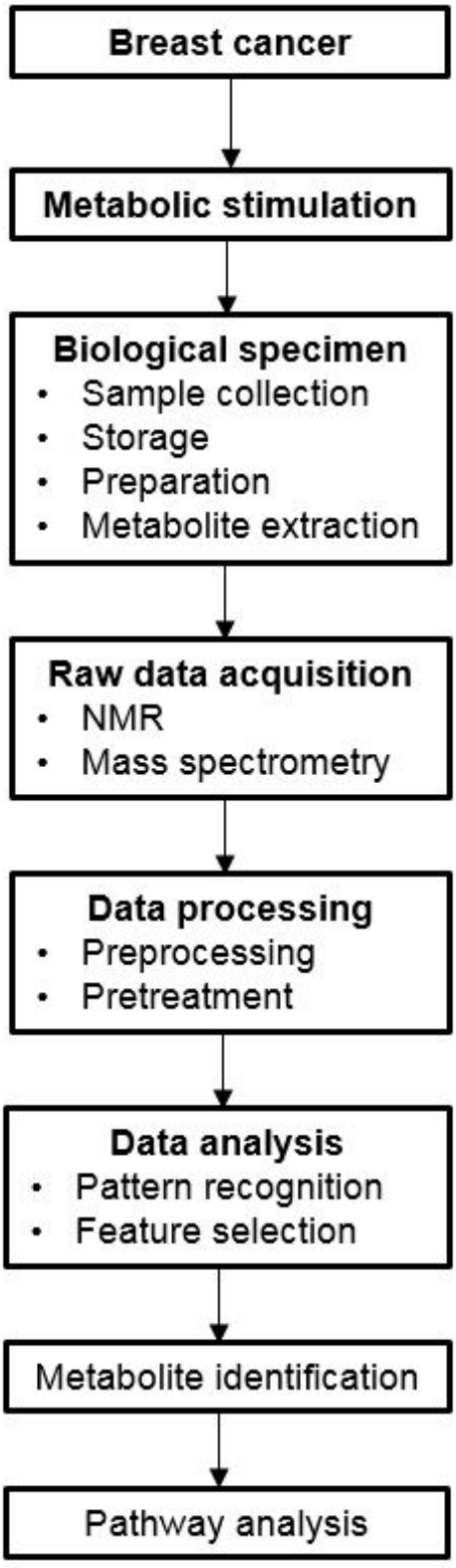

Fig. 1.9.: Flow sheet of metabolomics based experiment for breast cancer.

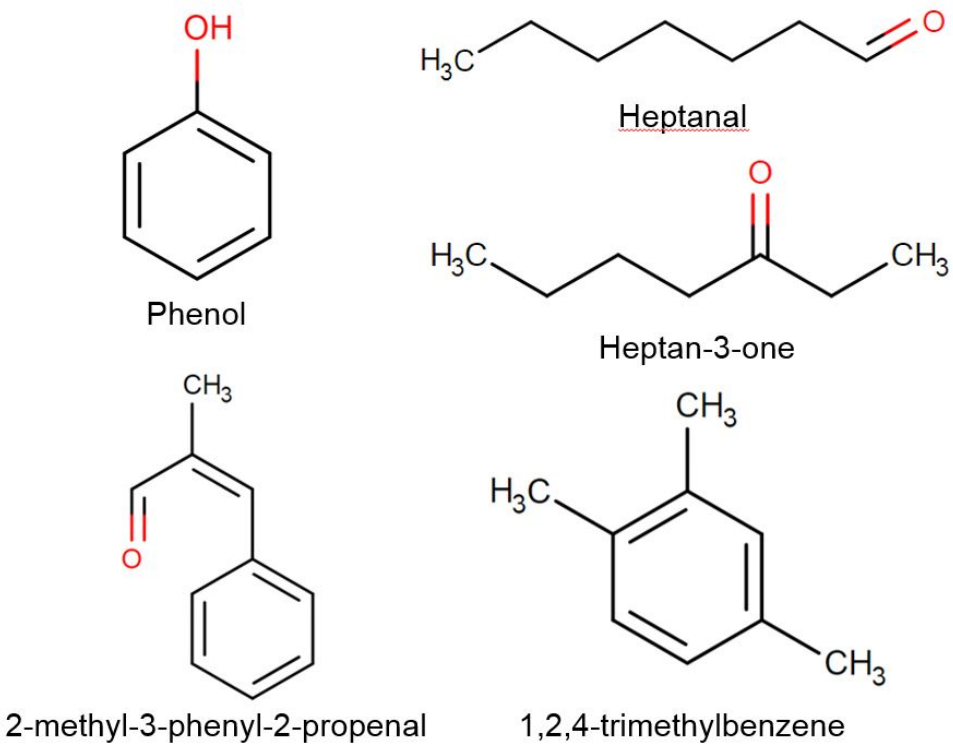

Fig. 1.10.: Chemical structures of VOC biomarkers for breast cancer identified from breath samples. [61–64]

distinguishing patients with and without breast cancer with 78.5% sensitivity and 84.8% specificity in their training data set [63]. Alternative method of biomarker discovery is through in vitro studies of breast cancer cell lines and healthy cultured cells [55, 56]. Experiments have shown the potential of VOCs biomarkers in other diverse disease types. Siavash et. al, published VOC biomarkers for diabetes identified using FAIMS and e-noses [65]. Khalid et. al, published a distinct set of VOCs specific to prostate cancer [66].

The novelty of this study is the reproducibility of potential breast cancer biomarkers across a series of experiments. Moreover, knowledge and data-driven based approach for supervised classification led to relevant biological interpretation. The hypothesis of this experiment is changes in VOC concentrations due to cancer can be

restored by therapeutic agents and their corresponding effect can be phenotypically observed with tumor size.

1.4.2 Urine as a VOC Source

Few breast cancer metabolomics studies previously demonstrated the prospective use of plasma, serum and tissue samples in distinguishing diseased subjects from healthy controls [67–70]. However, a major pitfall in their clinical applicability is the need of advanced technical development leading to expensive procedures. These tests also induce stress and uneasiness in patients similarly seen with the use of conventional techniques. Urine, on the other hand serves as an important tool in understanding bodys homeostasis [71]. The tendency of blood to undergo homeostatic control leads to transfer of metabolic changes to urine [72]. Furthermore, non-invasive sample collection allows for multiple time point collection of urine without affecting patients comfort and easy cost effective handling, storage and processing of urine qualifies it as an informative VOC source.

1.5 Question and Hypothesis

Prior studies have shown differential VOC profiles in subjects with breast cancer as compared to healthy control subjects. However, the reproducibility of these biomarkers and their corresponding biological interpretation is not well illustrated. The goal of this study is to address the question: Can urinary VOCs discern differences in oncogenic pathways and tumor locations with breast cancer pathogenesis and corresponding treatment options? To address this question, a series of experiments using in vivo models were conducted and urine samples were collected and analyzed before and after tumor cell injection and after chemical drug or mechanical stimulation treatment. The hypothesis is differential profiles of volatile metabolites are produced due to disruption of metabolic pathways with the advent of cancer and identification of these VOCs will help understand signaling pathways and tumor in-

teractions. VOC biomarkers can also track treatment efficacy and help in disease prognosis.

2. MATERIALS AND METHODS

2.1 In Vivo Analysis

2.1.1 Animal Preparation

Female BALB/c mice were purchased from Harlan Laboratories, Indianapolis, IN, USA while C57BL/6 mice were purchased from School of Science Institutional Animal Care and Use Committee, Indianapolis, IN, USA. 4T1.2 murine tumor cells were obtained from Dr. R. Anderson at the Peter MacCallum Cancer Institute and E0771 murine tumor cells were obtained from CH3 BioSystems. A5 osteocyte cell line was obtained from Anatomy and Cell Biology Laboratory, Indiana University School of Medicine.

2.1.2 Tumor Cell Injection

To mimic mammary pad confined breast tumor model, 4T1.2 cells (5.0×10^5 cells in 50μl PBS) were subcutaneously injected into the mammary fat pad of mice. For bone tumor model, female BALB/c mice were injected with 4T1.2 cells (1.0×10^5 cells in 50μl PBS) in the right iliac artery. Furthermore, in C57BL/6 mice, E0771 cells (5.0×10^5 cells in 50μl PBS) were injected in the left tibia. All injections were done by Dr. Shengzhi Liu and Yao Fan.

2.1.3 Treatments

Chemical and Biological

Treatment agents, Trifluoperazine, Fluophenazine were administered every day after tumor cell injection in female BALB/c mice at the site of tumor injection [73].

Mice were classified into three groups with mice receiving vehicle control (placebo) and mice treated with drugs (1mg/kg body weight in mammary pad tumor model and 2mg/kg body weight in bone tumor model.) Agents were administered daily by Yao Fan.

Pitavastatin drug was administered every day in female BALB/c mice model of bone tumor. Mice receiving drug (8mg/kg body weight) were classified as one treatment class and those receiving vehicle control were grouped as placebo class. Only mice receiving tumor cells were treated with chemical drugs. Pitavastatin was administered daily by Luqi Wang.

A biological treatment mode, A5 osteocyte cell line was injected using an insulin syringe (2.5×10^5 cells) in the left tibia at the the site of tumor cell injection in C57BL/6 mice model of bone tumor. A5 was administered by Yao Fan.

Mechanical

Tibial loading was conducted using Electro Force 3100 (Bose, Inc, Framingham, MA, USA) on two strains of mice model of bone tumor at the site of tumor injection. Animals were anesthetized before loading in an anesthetic induction chamber using 2.5% isoflurane and 1 ml/min flow rate. Loading of tumor bearing mice with 2N force comprised the medium loading class and mice with 5N loading force comprised the high loading class. The loads were applied in the axial direction with the left foot placed on a custom made piezoelectric, and both foot and the knee joint were fixed. The mice were loaded 5 minutes every day for three weeks using 2 N force (peak-to-peak) at 2 Hz. For the placebo group, animals were anesthetized for 5 minutes in the anesthetic induction chamber and carefully returned to the cage.

Knee loading was performed in C57BL/6 mice model of bone tumor with compressive strength applied lateral to the site of tumor injection. The experimental setup was similar to tibia loading experiment. Mechanical loading experiments were conducted by Aydin Jalali.

2.1.4 Urine Collection

All experimental procedures followed the Guiding Principles in the Care and Use of Animals supported by American Physiological Society and approved by Indiana University Animal Care and Use Committee. Mice were housed in glass cages at normal room temperature (25°C) and fed the same diet (mouse-chow ad libitum). Mice were moved to a cage covered in parafilm and given gentle abdominal pressure to facilitate urination. Urine was collected using pre-cleaned glass Pasteur pipettes into pre-cleaned 10 mL glass headspace vials. Urine was collected by Dr. Shengzhi Liu, Luqi Wang, Yao Fan and Yue Wang and assisted by Meghana Teli.

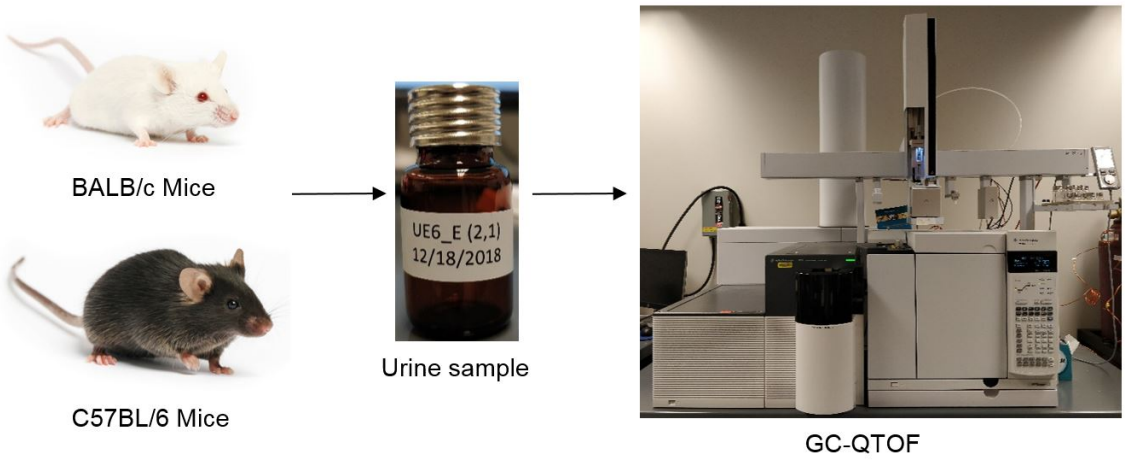

Fig. 2.1.: Mouse urine collection and analysis. Urine samples collected from BALB/c and C57BL/6 mice model of mammary pad and bone tumor model. Specimen analysis using gas chromatography-mass spectrometry quadruple time-of-flight (GC-MS QTOF).

2.2 Urine Analysis

2.2.1 Sample Preparation

Urine aliquots of 50μl were prepared from each sample and guanidine hydrochloride (8 M, Sigma Aldrich) was added in a 1:1 ratio (Figure 2.1.) Guanidine hydrochloride is used as a major urinary protein denaturing agent and to increase the ionic strength of the sample solution. Preliminary optimization experiments were conducted by Mark Woollam and Paula Angarita. All sample preparations were done by Meghana Teli.

2.2.2 SPME-GCMS

GC-MS is an analytical chemistry tool for analyzing volatile compounds comprising of two building blocks: a gas chromatograph and a mass spectrometer. GC and MS are used in conjunction to first differentiate compounds and then identify them by their mass spectral signatures. Chromatography separates molecules depending on their chemical properties. In GC, the mobile phase is a gas that carries molecules along a capillary column: depending on their affnity to the stationary phase, molecules will elute at different retention times. The molecules are eluted into the downstream mass spectrometer which ionizes and fragments them further for identification based on mass-to-charge ratios.

The QTOF-MS system is one such type of mass spectrometer detector that provides high quantification capability and mass accuracy of ions using a quadrupole, hexapole collision cell and time-of-flight. The sample is initially ionized with an electron impact (EI) ion source and resulting ions are filtered through quadrupole mass analyzer based on their mass to charge ratio (m/z). The filtered ions are directed to collision cell for further fragmentation into product ions before sending them to the fight tube. In the tube, an acceleration pulse is applied orthogonal to the direction of product ions. After reaching the end of the flight tube, ions are bounced off a

reflector and travel reverse path back down. The analog-to-digital detector counts ions and sends a signal for data collection. The same kinetic energy is given to all molecules in flight, however, the velocity of each molecule is a function of its mass. Heavier molecules will travel at a low speed and therefore, require more time to travel in the tube compared to lighter molecules. The mass determined is thus, accurate to the time taken to travel the length of the flight tube.

For this thesis work, urine was heated and agitated at 60°C for 30 minutes to release VOCs into the sample headspace. A pre-conditioned 2 cm PDMS/CAR/DVB SPME fiber (Supelco) was inserted through the septum of the vial for an additional 30-minute incubation at the same temperature and agitation to concentrate VOCs from the headspace. After incubation, the SPME fiber was inserted into the column inlet at 250°C for two minutes to thermally desorb VOCs (Figure 2.2.). Samples were analyzed and VOCs were detected using 7890A GC system coupled to an Agilent 7200 Accurate-Mass QTOF MS system with a PAL autosampling system (CTC Analytics). The chromatographic protocol involved the oven temperature maintaining 40°C for 2 minutes followed by a ramp to 100 °C at a rate of 8°C/min, followed by a 15 °C/min ramp to 120 °C, 8 °C/min to 180°C, 15 °C/min to 200°C and finally an 8°C/min ramp to 260°C. The column utilized was an Agilent HP-5ms, 5 % phenyl methyl siloxane GC column of 30 meters in length, 250 μm internal diameter and .25 m film thickness. Controls of standard urine (UTAK) were run daily and demonstrated consistency of measurements over the course of the experiment.

Methods for GC analysis were developed by Dr. Amanda Siegel, Mark Woollam. Samples were run on the GC-MS QTOF primarily by Meghana Teli, with assistance from Mark Woollam and Paula Angarita. All subsequent steps were performed by Meghana Teli with results reviewed by mentors and colleagues.

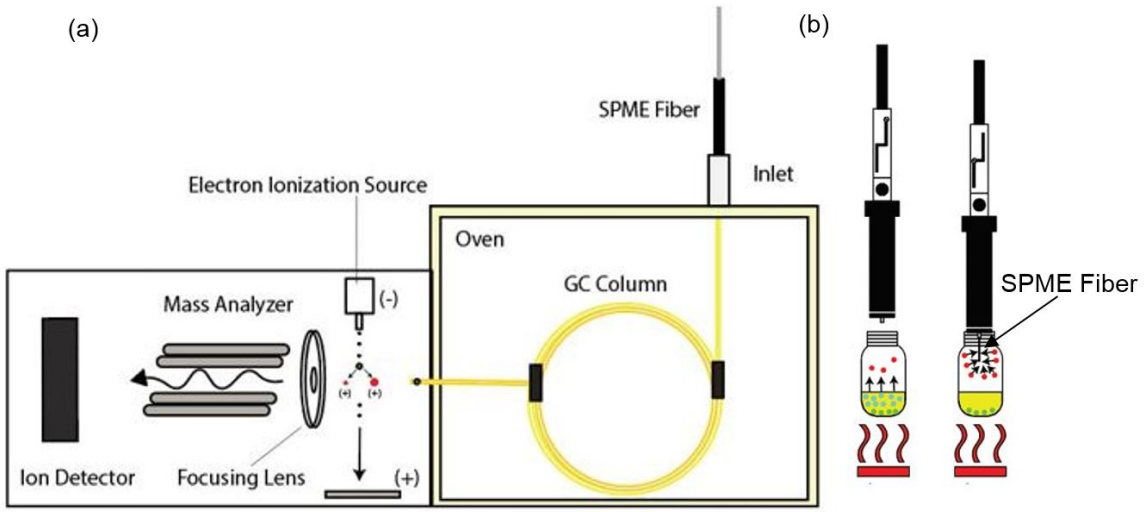

Fig. 2.2.: Illustration of GC-MS instrumentation (a)Analytes are eluted from gas column at different retention times, the MS system coupled to GC ionizes eluted analytes and filters them according to their mass-to-charge ratios before detection by the ion detector, (b) Solid phase microextraction utilizing fiber for headspace analysis of urine. Voltile organic compounds are transferred to the headspace of the vial after heating and agitation and adsorbed on the fiber.

2.3 Data Analysis

2.3.1 Data Pre-Processing and Pre-Treatment

GC-MS data were collected in centroid format (Figure 2.3.). Deconvolution and spectral alignment of multiple chromatographic peaks across all samples based on similarities of mass-to-charge (m/z) ratios and experimental retention times was performed using MassHunter Quantitative Profinder (version B.08.00) (Figure 2.4.). A matrix of compounds with integrated signal values and retention times for every sample was generated using the batch molecular feature extraction method. To account for differential intake of water in mice and rate of urine generation, a mass spectral total useful signal (MSTUS) approach was adopted for each VOC across all the samples [74]. It is equivalent to the ratio of integrated signal of a VOC in a sample to

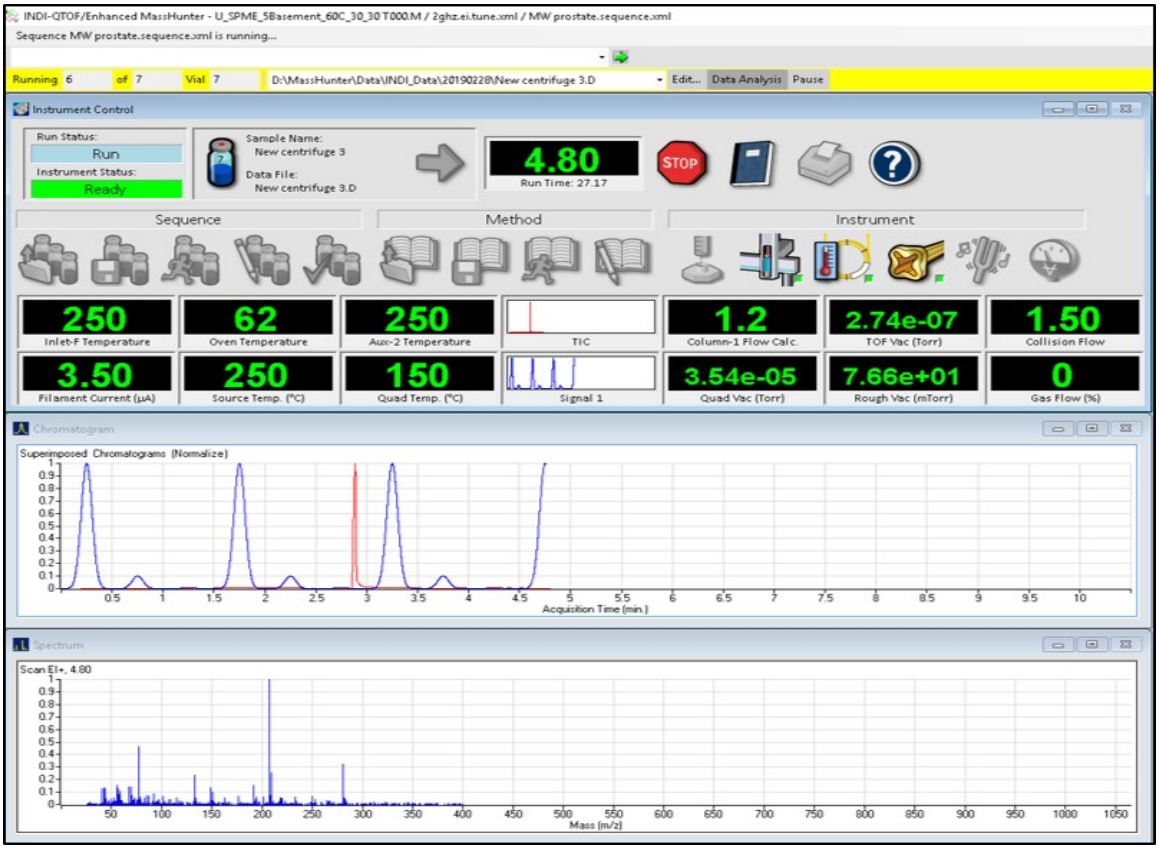

Fig. 2.3.: Snapshot of GC-MS QTOF data acquisition in Enhanced MassHunter software. The numbers in green are parameters of instrument operation such as oven temperature (62°C), filament current (3.5 microamperes), column flow rate (1.2%ml/min), run time (4.8 minutes). These indicate real-time functioning of the instrument. The chromatographic peaks are the elution profiles of mobile phase (blue) and analytes (red) with acqusition time. The lower panel depicts the mass-to-charge ratios of molecules and their counts as detected by the MS system.

the sum total integrated signal values of all VOCs in the same sample [74].The data were tested for normality distribution using skewness and kurtosis with the accepted limits of less than 1.96 [75, 76].

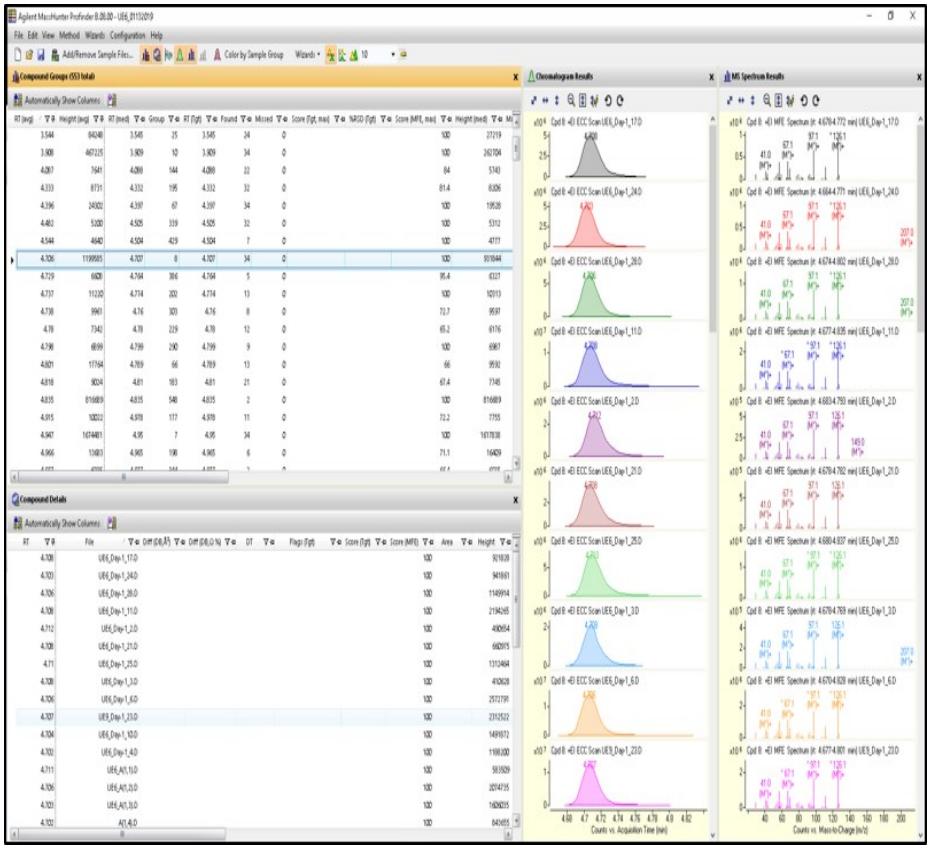

Fig. 2.4.: Snapshot of deconvolution and spectral alignment in MassHunter Profinder software. Deconvolution is separation of overlapping or co-eluting features based on their mass-to-charge ratios giving a list of compounds with given retention times and mass-to-charge ratios. Spectral alignment is comparing mass spectra for each feature across every sample.

2.3.2 Univariate Data Analysis

Univariate analysis was performed as a filter [77] using a two-tail Student's t-test (p value<0.05) on the VOCs present in at least 60% of at least one sample class to screen for VOCs differentially excreted between control and placebo sample class [58]. Scatterplots called volcano plots are used for large data to visualize global regulation patterns [78]. Herein, the log base 2 value of fold change (concentration of VOC in placebo class to concentration of VOC in control class) of metabolites between the control and placebo sample classes was calculated and plotted against negative log

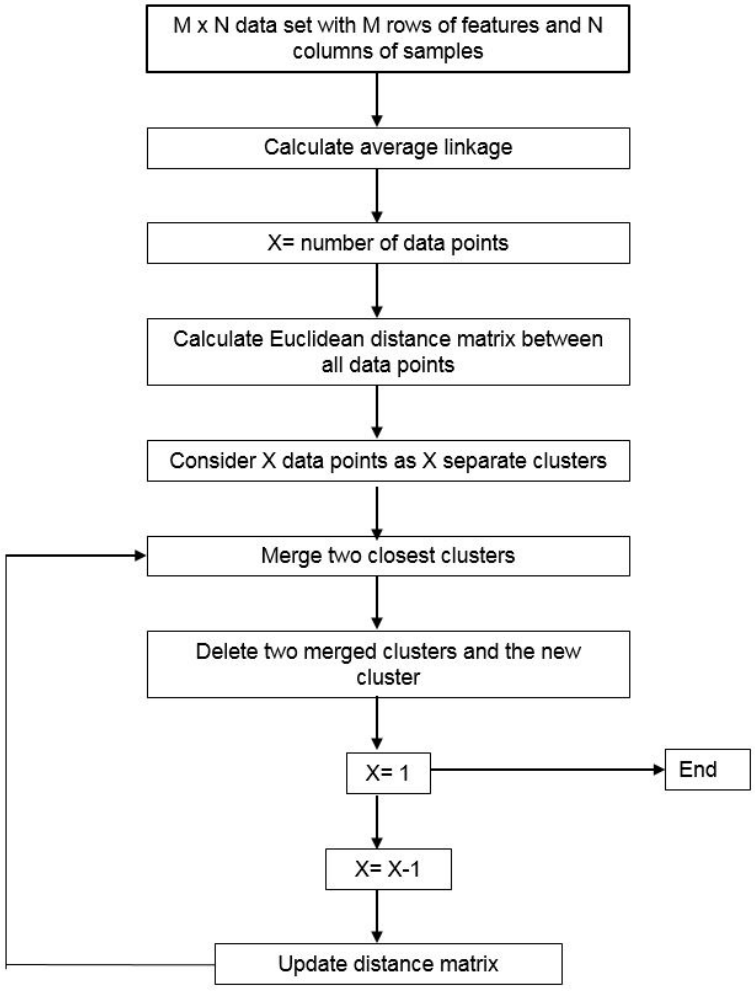

Fig. 2.5.: Flow-sheet of Hierarchical Clustering.

base 10 value of p-value given by Student's t-test to generate volcano plots for overall distribution of metabolites in both comparisons (mammary pad tumor or bone tumor with respect to control).

After a set of statistically significant features has been identified, a heat map of these compounds, ordered by hierarchical clustering can be generated to visually map concentration profiles of each sample and each VOC in an organized manner. Using the compounds identified above as statistically significant, hierarchical clustering in MATLAB (R2018b; Math Works) was undertaken for control, placebo and treatment classes. Hierarchical heat maps were created by z-scoring relative abundance values

for all VOCs across all samples (Figure 2.5.) [79]. Compounds are grouped based on their similarities in terms of concentration across all samples, and Euclidean distance metrics and average linkages were utilized to generate the hierarchical tree. Typically, compounds are on the y-axis and samples are along x-axis of the heat map. Data analysis procedures were conducted by Meghana Teli.

2.3.3 Compound Identification

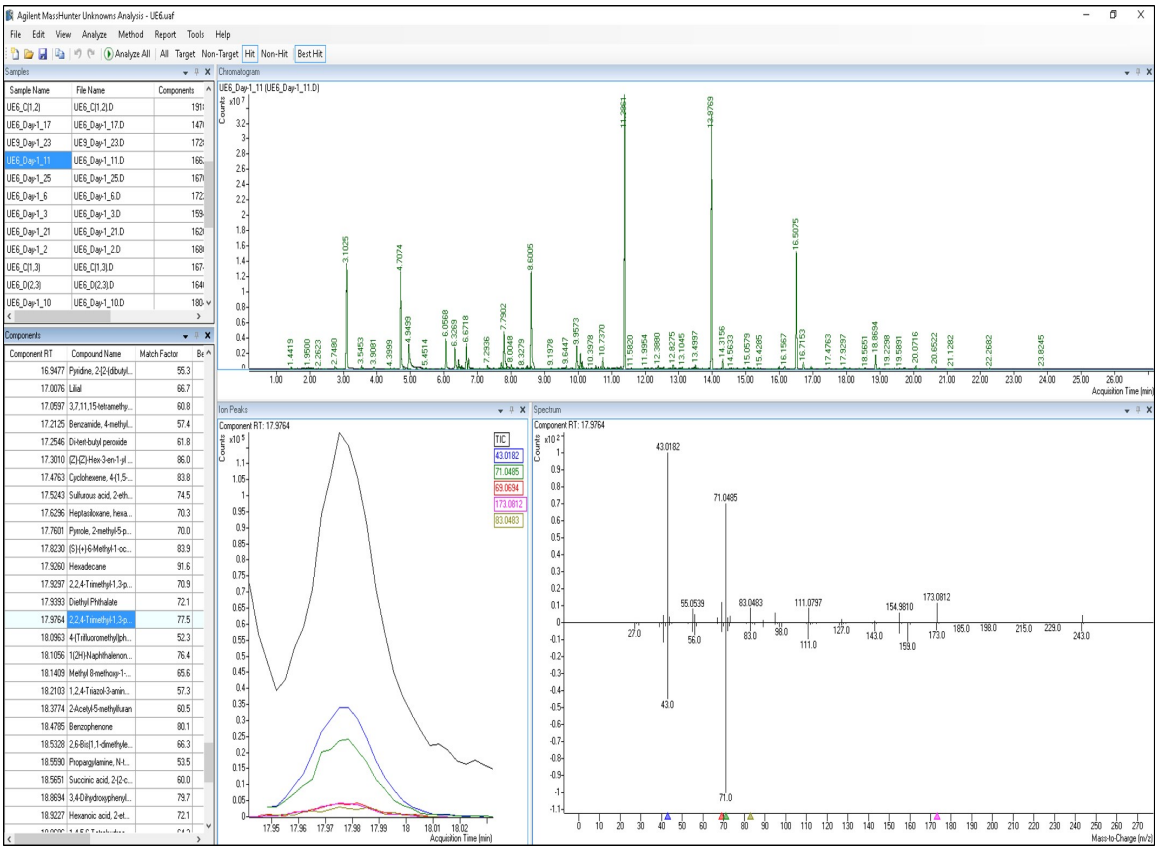

Fig. 2.6.: Snapshot of compound identification in Unknown Analysis by comparing mass spectra for every compound to the corresponding mass spectra obtained in MassHunter Profinder at a given retention time.

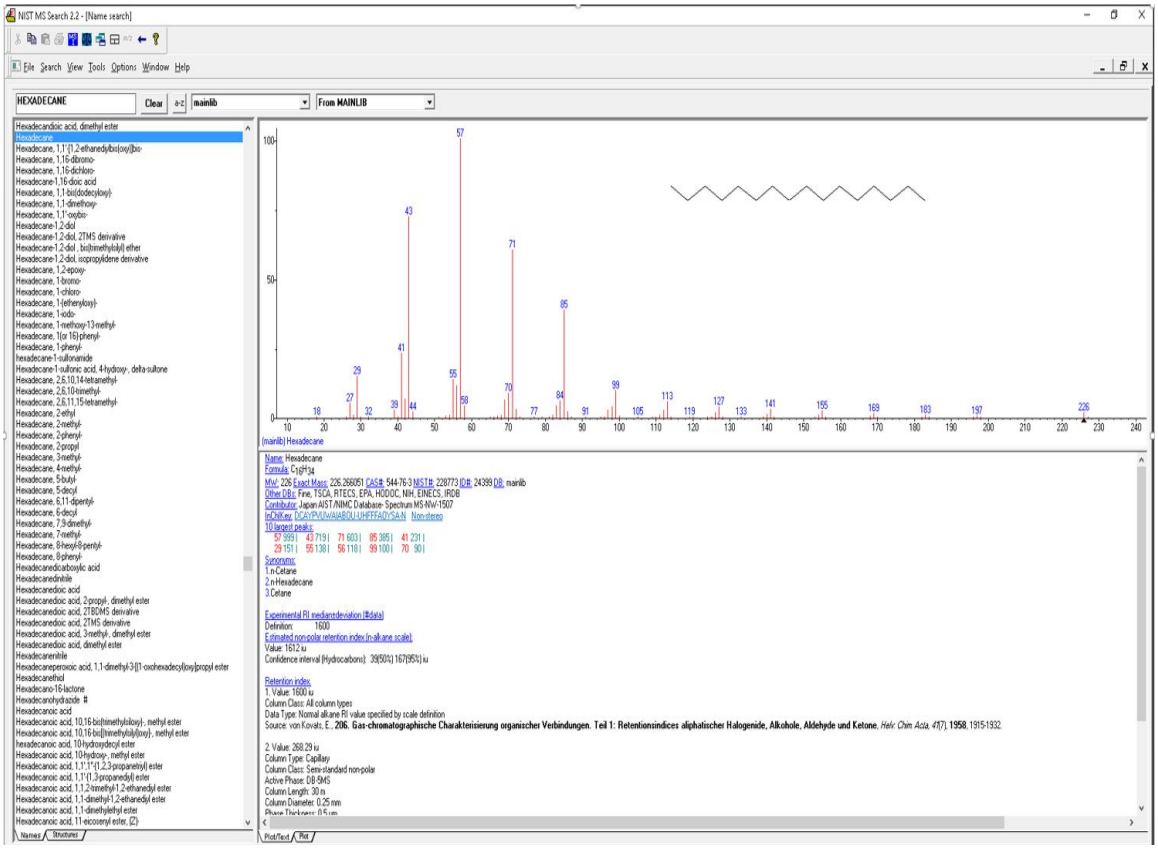

Fig. 2.7.: Snapshot of compound identification in NIST14, a mass-spectral library by comparing the given non-polar retention index to the calculated non-polar retention index.

Statistically significant VOCs (p value<0.05) were identified using Mass Hunter Quantitative Profinder and Mass Hunter Unknown Analysis (version B.08.00) integrated with the NIST14 mass spectral library. VOCs in Profinder were found in Unknown Analysis using the average retention times and mass spectra (Figure 2.6). Features identified with a match factor higher than 65 from the NIST library were initially identified. Preliminary confirmation of these compounds was performed by comparing the non-polar retention index (NPRI) given in NIST to the experimental NPRI value calculated from the average retention time (Figure 2.7). If both values were within the range of 100 units, the compound was deemed identified. Pure chem-

ical compounds were not analyzed via GC-MS QTOF to confirm the identification of potential VOC biomarkers.

2.3.4 Multivariate Data Analysis

Principal Component Analysis is a dimension reductionality technique used for visualizing complex data sets. The differences within the samples of the data set are observed along principal component axes. These are directions along which maximum variance in data is seen and are equal to eigen values of the covariance matrix. The highest variance is shown along principal component axis 1 followed by the second highest variation shown along principal component axis 2 and so on. PCA was conducted using statistically significant (p-value < 0.05) compounds in placebo and control classes to visualize global patterns when compared to treatment classes [80].

Supervised forward feature selection [81] was performed via iterative LDA [58] on features with p value < 0.05 to reduce data dimensionality and distinguish between placebo and control classes. It iterates the process of assigning a three-dimensional score for each sample for every permutation of VOCs tested. Effectiveness of each panel of VOCs was calculated by determining distance between the means for each class of samples divided by variance. The VOC panel producing maximum distance between the means of placebo and control classes via iterative LDA was selected until the panel gave perfect separation between groups (area under the receiver operating curve equal to one). LOOCV was performed to generate a cross-validated AUROC and to test if the classification models are over fit [34]. The results of LDA were plotted to visualize the separation between groups using the VOC panel selected. Next, samples receiving treatment were plotted in the same dimensional space transformation to test if the samples reflect tumor bearing or control mice. The Variation Inflation Factor (VIF) was calculated to assess the degree of multicollinearity present in each classification model [40]. A VIF threshold value of 10 was employed as a cut-off value to indicate a high degree of multicollinearity between predictor and response

values [35, 82]. MATLAB algorithms and data analysis procedures were augmented by Dr. Amanda Siegel, Dr. Ali Daneshkhah, Sanskar Thakur and Mark Woollam.

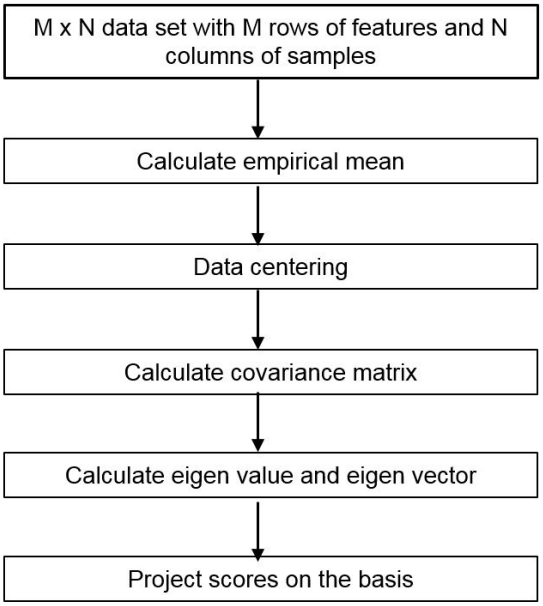

Fig. 2.8.: Flowsheet of Principal Component Analysis.

3. RESULTS

3.1 Urine Collection

Collection of urine specimens from BALB/c mice and C57BL/6 mice is summarized in Table 3.1. Twenty-four BALB/c mice were injected with 4T1.2 cells in the mammary fat pad, eight of which received no treatment (placebo), and eight received Fluphenazine treatment agent and the other eight received the Trifluoperazine treatment agent.

A different set of fifty-three mice were injected with 4T1.2 cells in the iliac artery to induce bone tumor and twenty-six received no treatment, nine received Fluphenazine treatment agent, seven received Trifluoperazine treatment agent and eleven were treated with Pitavastatin. Mechanical loading in tibia was conducted on another set of twelve mice. Similarly, for C57BL/6 mice injected with tumor cells, ten received vehicle control, four received 2N loading in the tibia, six received 5N loading in the tibia and a different set of mice received knee loading treatment lateral to the site of tumor injection. Additionally, six different mice were treated with A5 osteocyte cell line . All control samples in the experiments were obtained before mice were injected with tumor cells to form the healthy control class.

3.2 Data Pre-Processing and Pre-Treatment

Samples analyzed by GCMS QTOF resulted in acquisition of centroid-based GCMS data files. A matrix for every data set consisted of compounds extracted on the basis of average retention times ranging from zero to twenty-seven minutes and having an average peak height of greater than 500 counts. VOCs with standard deviation in retention times less than 0.8 minutes of the average retention times were included

Table 3.1.
Number of Urine Samples For Each Study

Model	Treatment	Number of mice
Mammary Pad Model in BALB/c Mice	Control	5
	Placebo	8
	Fluphenazine	8
	Trifluoperazine	8
Bone Tumor Model in BALB/c Mice	Control	37
	Placebo	26
	Fluphenazine	9
	Trifluoperazine	7
	Pitavastatin	11
	Tibia loading (5N)	12
Bone Tumor Model in C57BL/6 Mice	Control	22
	Placebo	10
	Tibia loading (2N)	4
	A5	6
	Tibia loading (5N)	6
	Knee loading	7

in the matrix. Simultaneously, VOCs having a relative molecular feature extraction score of greater than 65% formulated the matrix.

3.3 Effect of Tumor Site on VOCs

For the mammary pad tumor model, a matrix with 215 compounds present in at least 60% of either control or placebo class after removing compounds characteristic of SPME fiber or column degradation was generated. Similarly, for bone tumor model, a matrix comprising of 370 compounds was generated. The data had a normal

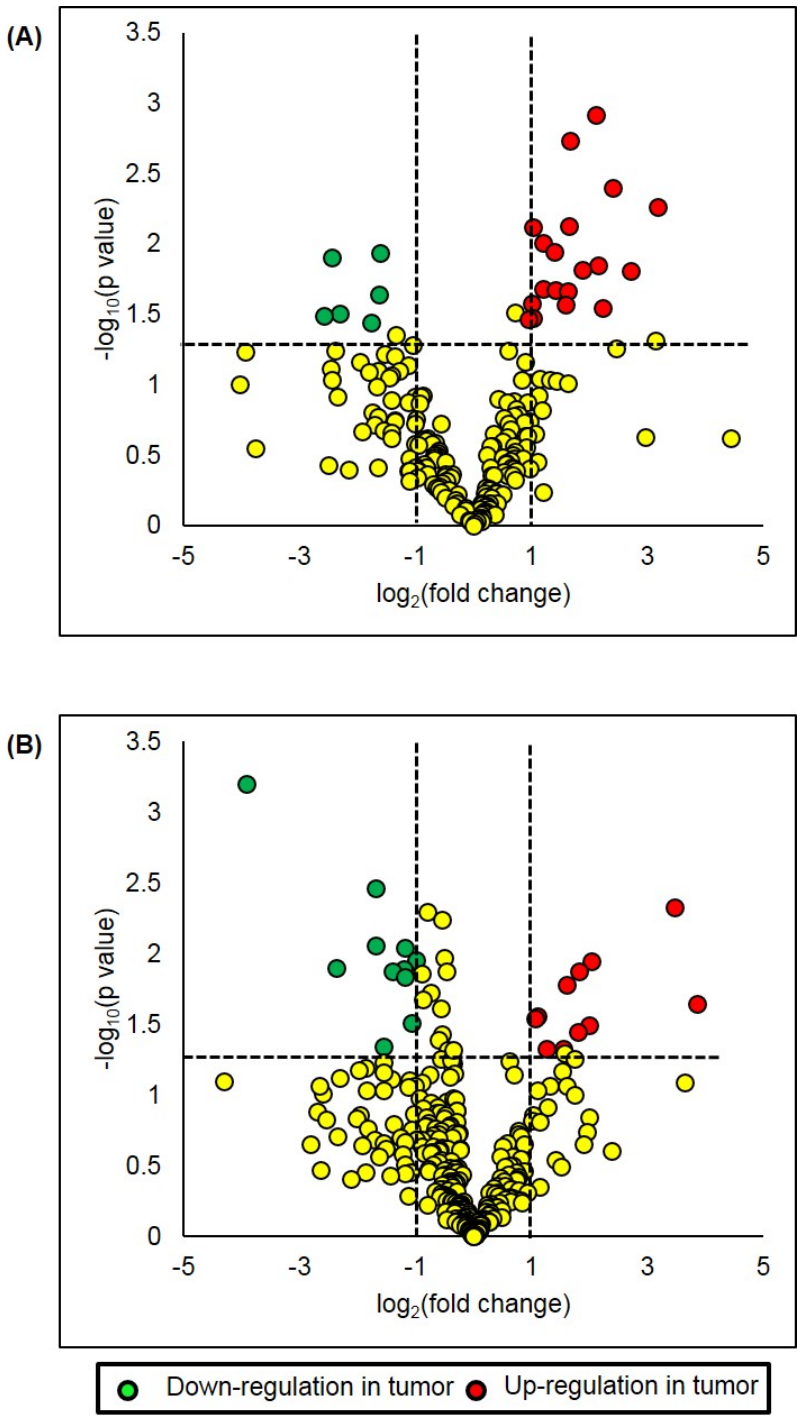

Fig. 3.1.: Volcano plots for overall distribution of urinary VOCs (yellow) in BALB/c mice model of (A) mammary pad tumor (n=8) compared to control (n=5), (B) bone tumor (n=7) compared to control (n=6). Negative log of p-value from Student's t-test plotted as a function of $\log_2$ fold change. Fold change is the ratio of concentration of a VOC in tumor class to control class. VOCs above the horizontal line are statistically significant (p value$<$0.05) while VOCs with absolute fold change of 1 are located after x=$\pm$1).

distribution with z-score values for skewness and kurtosis. Volcano plots for both comparisons (mammary pad or bone tumor models with respect to controls) can be observed in Figure 3.1., compounds with positive $\log_2$fold change are seen to be up-regulated. VOCs with an average absolute $\log_2$fold change greater than one and p-value < 0.05 (T-test) are colored green (down-regulated in cancer) or red (up-regulated in cancer).

Of those VOCs differentiating between mammary pad tumor model and controls , seventeen are up-regulated and seven are down-regulated in cancer. For bone tumor and control models, nine VOCs were observed to be up regulated and twenty-one VOCs were down regulated in cancer. Students t-test alone gave a total of twenty-four VOCs different between control and mammary pad tumor classes and thirty between control and bone tumor classes (p value <0.05). Tables 3.2. and 3.3. contain, for each VOC in the two data sets, a VOC ID number, a colloquial name and IUPAC name, CAS ID, p-value). The VOCs in Tables 3.2. and 3.3. were further analyzed in mice receiving the two treatment agents to observe their ability to monitor treatment efficacy.

VOCs identified from univariate analysis had a variety of functional groups and structural features. Terpenes are precursors of cholesterol/steroids and were identified both in mammary pad or bone tumor models. Following Xia, knowledge and data driven based feature selection methods were utilized for iterative LDA (41) by utilizing VOCs related to the mevalonate pathway and compounds previously identified as potential markers for breast cancer. For the mammary pad tumor model, a panel of four VOCs (d-limonene, isoprene, isoprenyl alcohol, p-menth-3-ene) provided separation between control and placebo as seen in Figure 2.3. (a). LOOCV was utilized to test if the classification model was over fit, and produced an estimated AUROC of .93 for the mammary pad tumor model comparison with respect to controls. The VIF calculated for predictor and response values was 2.04 (low), demonstrating non-collinearity of compounds. For the bone tumor model, a different set of three VOCs (octa-1,3-diene, 2,4,4-trimethyl-3-(3-methylbutyl) cyclohex-2-en-1-one, nerol)

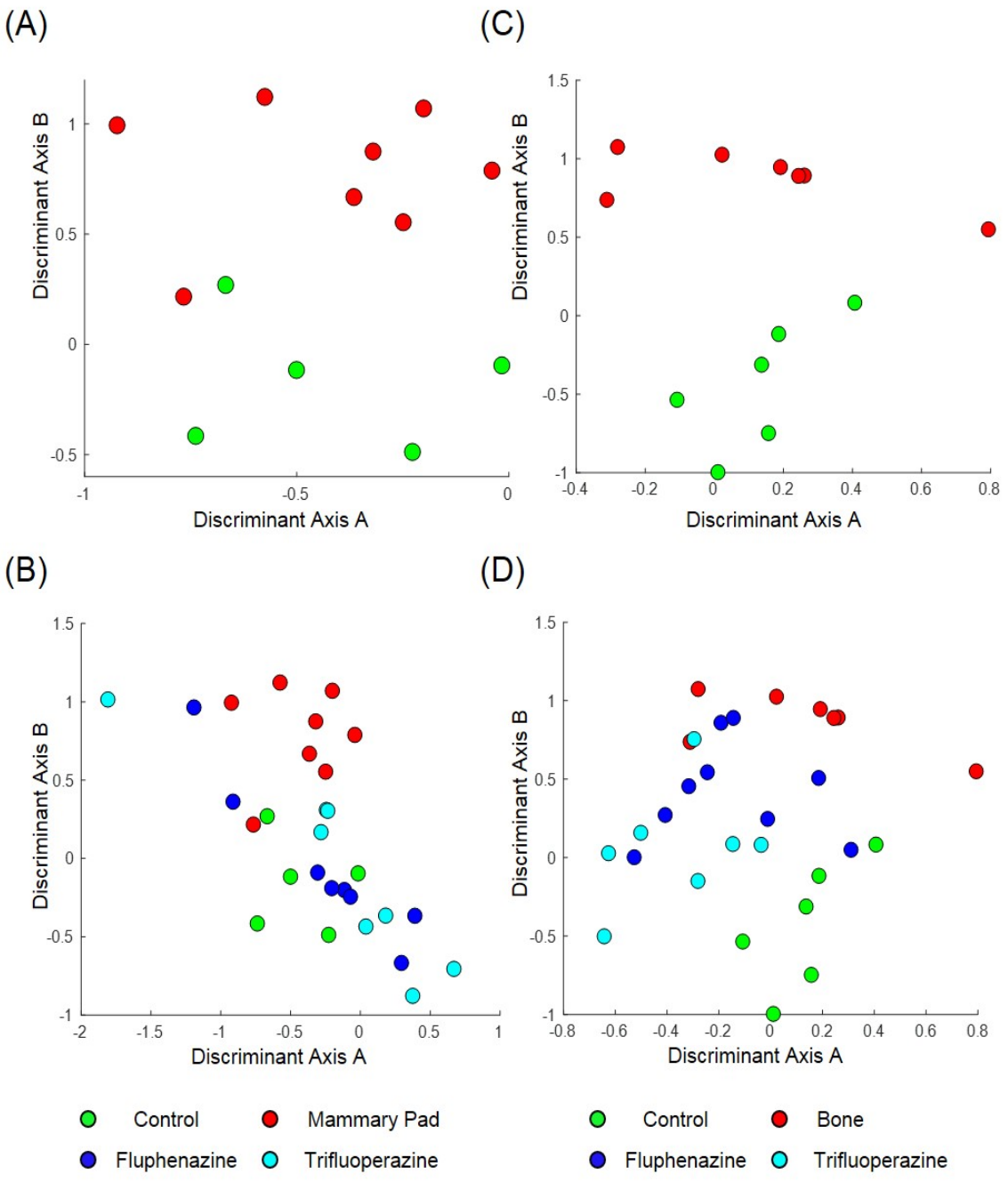

Fig. 3.2.: Iterative linear discriminant analysis for (A) mammary pad tumor model with compound ID 3, 2, 7, 19 (from Table 3.2) with (B) both treatments plotted on the first two linear discriminant axes, and (C) bone tumor model with compound ID 1, 20, 27(from Table 3.3 and 3.4) with (D) both treatments plotted on the first two linear discriminant axes.

Table 3.2.
IUPAC Names of VOCs Statistically Significant in Mammary Pad Model

VOC ID	IUPAC (Common names)	CAS ID	P value
1	2,5-ditert-butylcyclohexa-2,5-diene-1,4-dione	2460-77-7	0.032
2	(4∼{R})-1-methyl-4-prop-1-en-2-ylcyclohexene	5989-27-5	0.012
3	penta-1,4-diene	591-93-5	0.031
4	2,6-dimethylcyclohexan-1-ol	5337-72-4	0.036
5	1-(1∼{H}-pyrrol-3-yl)ethanone	1072-82-8	0.022
6	3-[(3,5-difluoro-4-hydroxyphenyl)methyl]) -1∼{H}-imidazole-2-thione	20290-99-7	0.011
7	2-methylbut-3-en-2-ol (Isoprenyl alcohol)	115-18-4	0.044
8	6-methyltridecane	13287-21-3	0.031
9	2-methylcyclopentan-1-ol	24070-77-7	0.034
10	(3E,5E)-octa-3,5-dien-2-ol	69668-82-2	0.026
11	nonanoic acid (Pelargonic acid)	112-05-0	0.033
12	2-ethylhexan-1-ol	104-76-7	0.009
13	1-methoxy-4-methylbicyclo[2.2.2]octane	6555-95-9	0.021
14	2,6,6-trimethylcyclohex-2-ene-1,4-dione	1125-21-9	0.011
15	Cyclohexanecarboxylic acid, 3-fluorophenyl ester	-	0.027
16	oct-1-en-3-one	4312-99-6	0.022
17	2-methylaniline	95-53-4	0.007
18	1,2,3,4-tetrahydroquinoline (Kusol)	635-46-1	0.001
19	4-methyl-1-propan-2-ylcyclohexene (p-menth-3-ene)	500-00-5	0.015
20	decanal	112-31-2	0.001
21	2-methylnon-2-en-4-one	2903-23-3	0.014
22	3-ethyl-2,5-dimethylhexa-1,3-diene	62338-07-2	0.015
23	2,6-dimethylcyclohexan-1-ol	5337-72-4	0.048
24	N,N-dimethylmethanamine	75-50-3	0.005

Table 3.3.
IUPAC Names of VOCs Statistically Significant in Bone Tumor Model

VOC ID	IUPAC (Common names)	CAS ID	P value
1	octa-1,3-diene	1002-33-1	0.0006
2	1,4-dimethoxybenzene	150-78-7	0.012
3	cyclooctene	931-89-5	0.003
4	4-propan-2-ylcyclohex-2-en-1-one	500-02-7	0.008
5	1-Octen-3-ol	13475-82-6	0.045
6	2,4-dimethylheptan-3-one	18641-71-9	0.013
7	2-hydroxy-3-propan-2-ylcyclohepta-2,4,6-trien-1-one	122-84-9	0.013
8	dec-3-en-5-one	32064-73-6	0.009
9	4-(2,5,6,6-tetramethylcyclohex-2-en-1-yl) but-3-en-2-one	79-69-6	0.031
10	3-methylhexanal	19269-28-4	0.011
11	1-methyl-4-(6-methylhepta-2,5-dien-2-yl) cyclohexene	25532-79-0	0.014
12	hexan-2-one	30637-87-7	0.021
13	butan-2-one	78-93-3	.005
14	(3E)-5-Methyl-3-undecene	-	.019
15	3-methylbenzaldehyde	620-23-5	0.04
16	1-(3,5-ditert-butyl-4-hydroxyphenyl)propan-1-one	-	0.024
17	(1Z,4Z,7Z)-1,5,9,9-tetramethylcyclo undeca-1,4,7-triene	-	0.037
18	[(Z)-hex-3-enyl] pentanoate	35852-46-1	0.005
19	(1E)-1-(3,5,5-trimethylcyclohex-2-en-1-ylidene) propan-2-one	3211-80-1	0.013
20	2,4,4-trimethyl-3-(3-methylbutyl)cyclo hex-2-en-1-one	-	0.047

Table 3.4.
IUPAC Names of VOCs Statistically Significant in Bone Tumor Model

VOC ID	IUPAC (Common names)	CAS ID	P value
21	1-(2,4,6-trimethylphenyl)ethanone	1667-01-2	0.048
22	1,2-dihydropyrazolo[3,4-d]pyrimidine-4,6-dione	2465-59-0	0.029
23	pentan-2-one	107-87-9	0.027
24	methoxycycloheptane	42604-04-6	0.047
25	2-ethylhex-2-enal	88288-45-3	0.047
26	7-methylthieno(3,2-b)pyridine	13362-83-9	0.016
27	(2Z)-3,7-dimethylocta-2,6-dien-1-ol (nerol)	106-25-2	0.035
28	(2E)-3,7-dimethylocta-2,6-dienal (geranial)	147060-73-9	0.013
29	Methyl (E)-but-2-enoate (methyl crotonate)	6709-39-3	0.011
30	4,5-dimethylhex-4-en-3-one	17325-90-5	0.022

provided perfect classification of samples from control and bone tumor bearing mice (Figure 3.2. (b)). Again, LOOCV was applied and produced an AUROC of .93. The VIF calculated for predictor and response values was 2.7, again demonstrating non-collinearity.

3.4 Effect of Chemical Treatment

The effect of agents, Trifluoperazine and Fluphenazine were analyzed using hierarchical heatmaps of VOCs listed in Tables 3.2. and 3.3 to show relative concentration of VOCs in the four groups: control, placebo (mammary pad in Table 3.2.or bone tumor in Table 3.3), Fluphenazine and Trifluoperazine (Figure 3.2.). The corresponding compound names associated with each VOC ID present in the hierarchical heatmap on the y axis can be found in Tables 3.2. and 3.3.

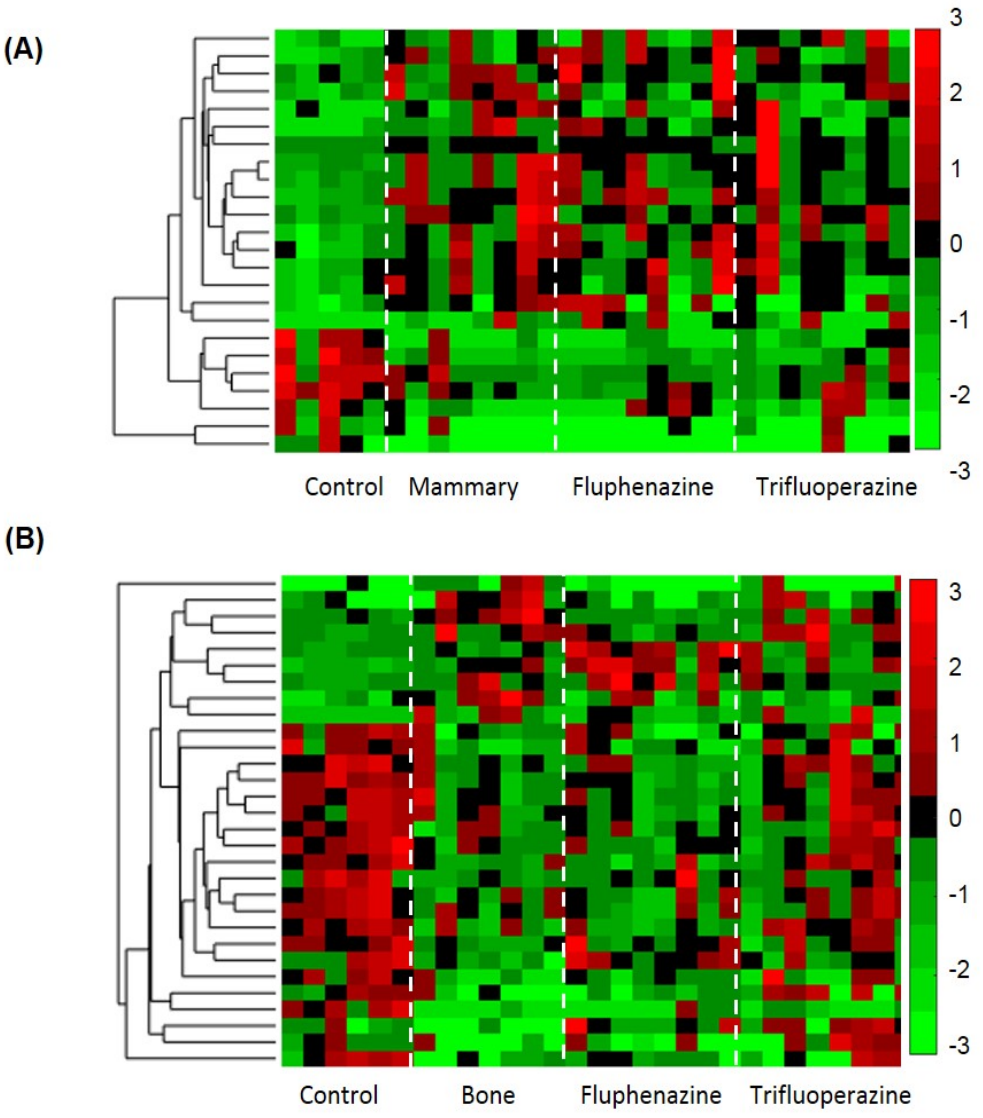

Fig. 3.3.: Hierarchical clustering of statistically significant features (p value<0.05) in placebo and control groups to understand the change in their concentration profiles in urine from mice treated for cancer in (A) mammary pad (n=8) and control (n=5) (24 features) with Fluphenazine (n=8) and Trifluoperazine (n=8), (B) bone tumor models (n=7) and control (n=6) (30 features) with Fluphenazine (n=9) and Trifluoperazine (n=7). Samples are across x-axis and VOCs across y-axis.

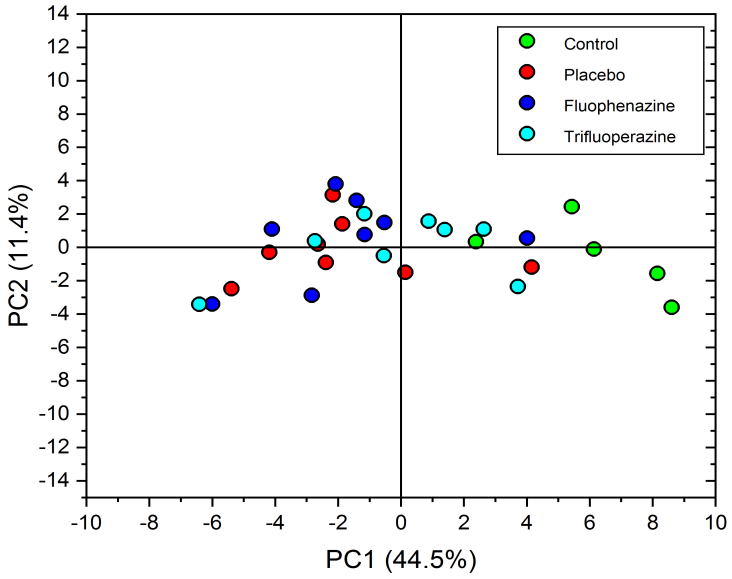

Fig. 3.4.: Principal component analysis of features (p value<0.05) in mammary pad tumor of BALB/c mice model (n=8) and controls (n=5) (24 features) to visualize global patterns with the effect of Fluphenazine (n=8) and Trifluoperazine (n=8) treatment.

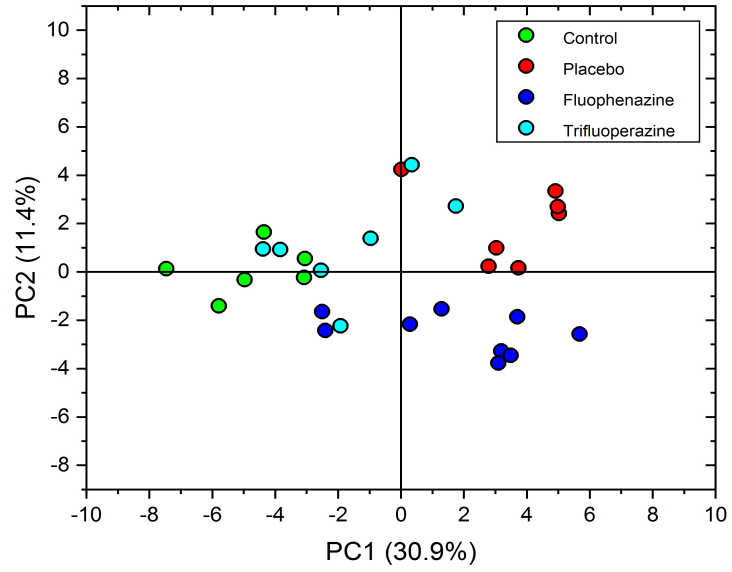

Fig. 3.5.: Principal component analysis of features (p value<0.05) in bone tumor model of BALB/c mice (n=7) and controls (n=6) (24 features) to visualize global patterns with the effect of Fluphenazine (n=9) and Trifluoperazine (n=7) treatment.

VOC concentrations in the urine of mice treated with Trifluoperazine looked more like control than mice treatment with Fluphenazine regardless of tumor injection location (mammary pad or iliac artery). However, mice injected with tumor cells in the iliac artery (bone) showed VOCs more similar to control mice for both treatments relative to mice injected into the mammary fat pad (mammary pad).

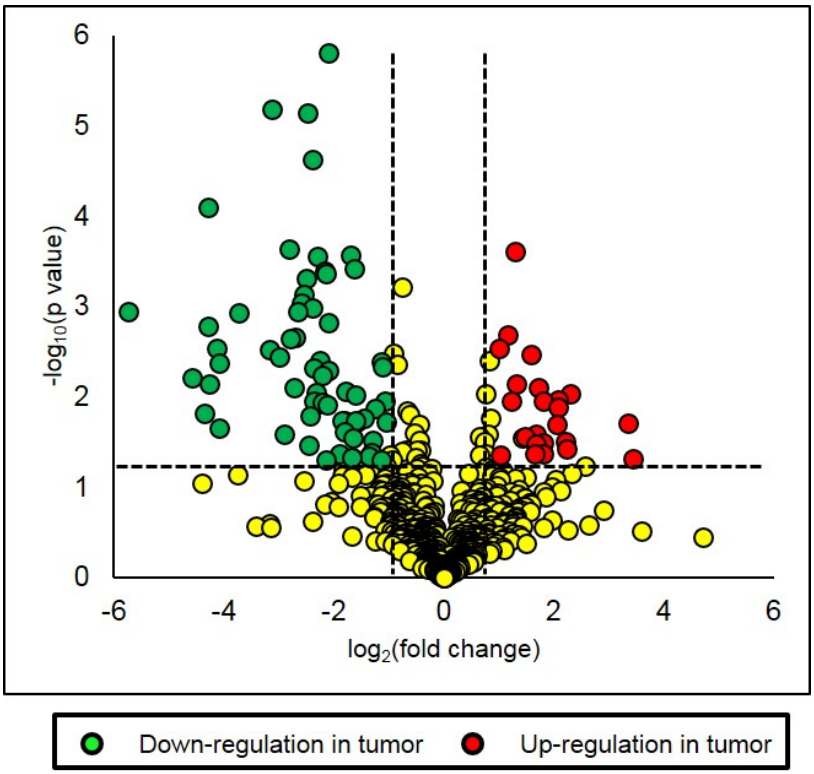

Fig. 3.6.: Volcano plots for overall distribution of 748 urinary VOCs (yellow) in BALB/c mice model of bone tumor (n=8) compared to control (n=20). Negative log of p-value from Student's t-test plotted as a function of $\log_2$ fold change. Fold change is the ratio of concentration of a VOC in tumor class to control class. VOCs above the horizontal line are statistically significant (p value$<$0.05) while VOCs with absolute fold change of 1 are located after x=$\pm$1).

Features identified and filtered through univariate statistics were analyzed using dimensionality reduction multivariate statistical tools. PCA was initially implemented using all the compounds listed in Tables 3.2. and 3.3. to visualize global patterns. For both comparisons, all four sample classes (control, placebo, TFP treat-

ment and FP treatment) are plotted along principal component (PC) axes 1 and 2 in Figure 3.4 and 3.5. The first two principal components in Figure 3.4. account for 56.2% of sample variation and 42.3% of variation in Figure 3.5. Both PCA plots demonstrated absence of sample outliers. PCA also shows similarity between control samples and samples treated with TFP relative to FP in mice with tumors in mammary pad or bone.

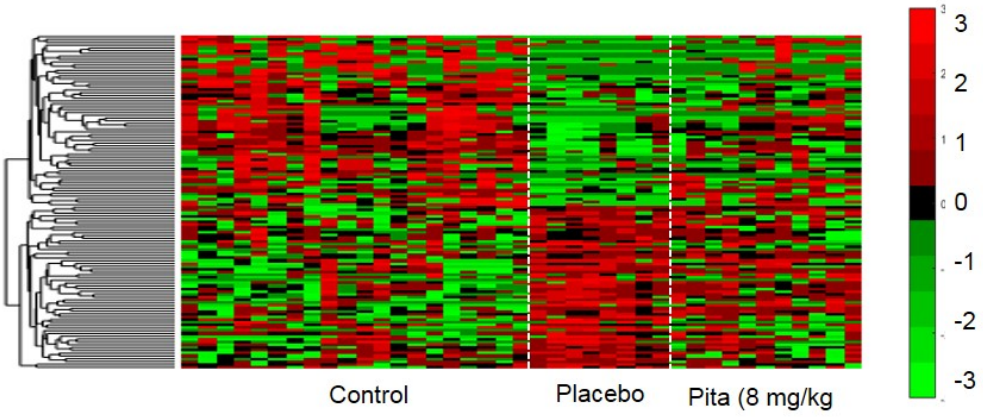

Fig. 3.7.: Hierarchical clustering of statistically significant features (p value<0.05) in placebo and control groups to understand the change in their concentration profiles in urine from bone tumor model of BALB/c mice (n=8) and control (n=20) (119 features) with Pitavastatin (n=11). Samples are across x-axis and VOCs across y-axis.

Efficacy of Pitavastatin was studied in bone tumor model of BALB/c mice using a matrix of 748 VOCs present in at least 60% of either control (n=20) or placebo (n=8) class and after eliminating compounds characteristic of SPME fiber or column degradation. Students t-test gave 114 VOCs statistically significant (p value<0.05) between control and placebo class.

Hierarchical heatmaps show the relative change brought by the Pitavastatin treatment on these cancers associated VOCs. Compounds up-regulated in the cancer class are observed to be restored to their original expression levels by the action of Pitavastatin.

Table 3.5.
IUPAC Names of VOCs Satistically Significant in Pitavastatin Study

VOC ID	IUPAC (Common names)	CAS ID	P-value
1	[2,2,4-trimethyl-3-(2-methylpropanoyloxy)pentyl] 2-methylpropanoate	6846-50-0	0.353
2	2-methylbut-3-en-2-ol	115-18-4	0.310
3	pent-3-en-2-ol	1569-50-2	0.048
4	5-methylheptan-1-ol	7212-53-5	0.019
5	5-ethylcyclopentene-1-carbaldehyde	36431-60-4	0.180
6	2-(4-ethoxyphenyl)-2-methylpropanal	-	0.259
7	1,3,5-trichlorobenzene	108-70-3	0.058
8	2-butan-2-yloxycarbonylbenzoic acid	53623-59-9	0.071
9	ethyl 4-ethoxybenzoate	23676-09-7	0.009
10	Toluene	108-88-3	0.299
11	1-methoxy-4-(1-methylpropyl)benzene	-	0.037
12	chlorobenzene	108-90-7	0.031
13	1,4-dimethoxybenzene	150-78-7	0.110
14	2-methoxy-4-methyl-1-pentylbenzene	-	0.010
15	Benzaldehyde	100-52-7	0.013
16	1-tert-butyl-4-methoxybenzene	5396-38-3	0.020
17	[3,6-dimethyl-3a,4,5,7a-tetrahydro-3H-1-benzo furan-2-one	57743-63-2	0.083
18	formyl benzoate	-	0.098
19	methylsulfonylmethylbenzene	3112-90-1	0.232
20	Benzoic acid	65-85-0	0.127
21	2-(Acetyloxy)tetrahydro-2H-pyran-3-yl acetate	-	0.011
22	Dimethyl 4-methoxyphenyl phosphate	7357-14-4	0.032
23	1-(4-hydroxy-3-methoxyphenyl)ethanone	-	0.043

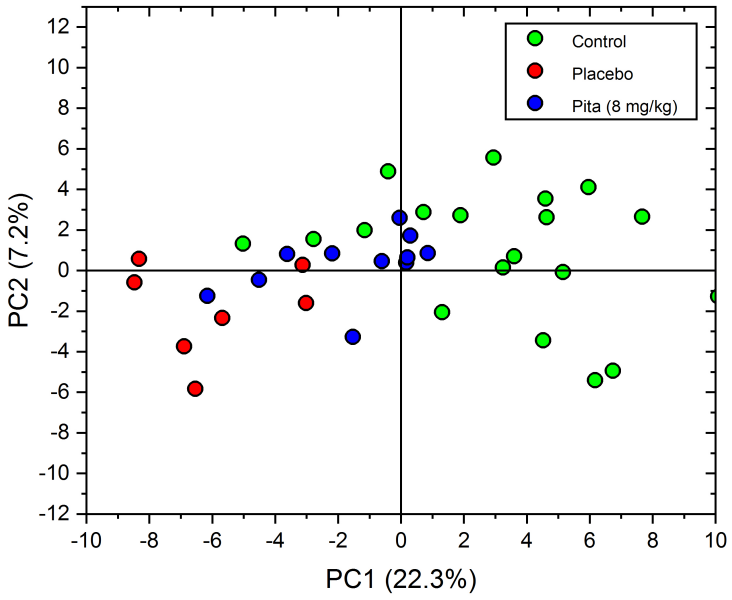

Fig. 3.8.: Principal component analysis of features (p value<0.05) in bone tumor model of BALB/c mice (n=20) and controls (n=8) (20 features) to visualize global patterns with the effect of Pitavastatin (n=11) treatment.

VOCs with top twenty p-values (<0.05) were utilized for clustering analysis to gain an understanding of treatment related change on p-value confirmed potential biomarkers. Consequently, PCA depicts overall reinstating of these VOCs from placebo towards control class (Figure 3.8.). The corresponding compound names associated with each VOC ID in Figure 3.8. are given in Tables 3.4.

3.5 Effect of Mechanical Treatment

Effectiveness of tibia loading on bone tumor model in C57BL/6 and BALB/c mice was investigated by monitoring differences in cancer associated VOCs. Matrices of 531 (C57BL/6) and 581 (BALB/c) VOCs with control, placebo and mechanically loaded classes were generated.

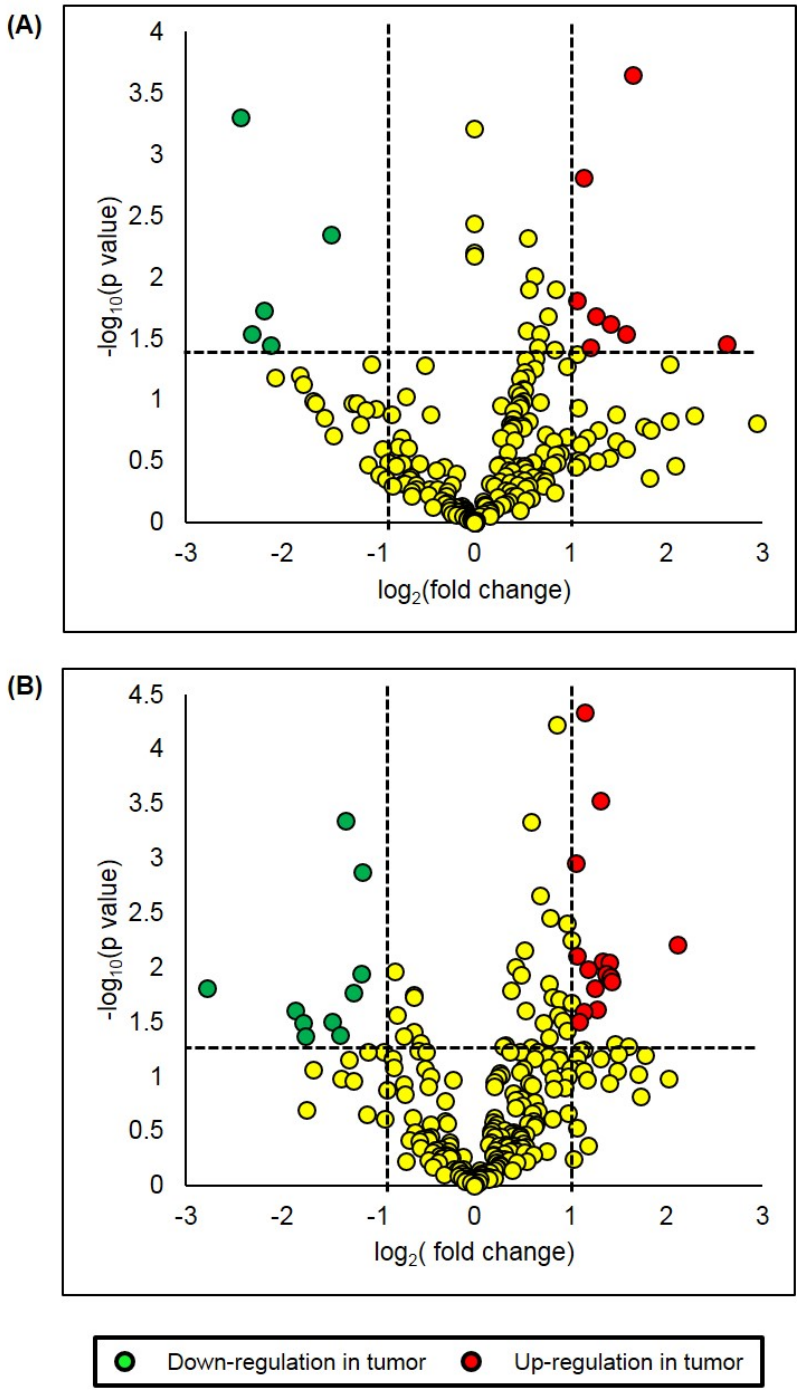

Fig. 3.9.: Volcano plots for overall distribution of urinary VOCs (yellow) in (A) BALB/c mice model of bone tumor with 531 features (n=12) compared to control (n=13), (B) C57BL/6 mice model of bone tumor with 581 features (n= 4) compared to control (n= 10) for Tibia loading study. Negative log of p-value from Student's t-test plotted as a function of $\log_2$ fold change. Fold change is the ratio of concentration of a VOC in tumor class to control class. VOCs above the horizontal line are statistically significant (p value$<$0.05) while VOCs with absolute fold change of 1 are located after x=$\pm$1).

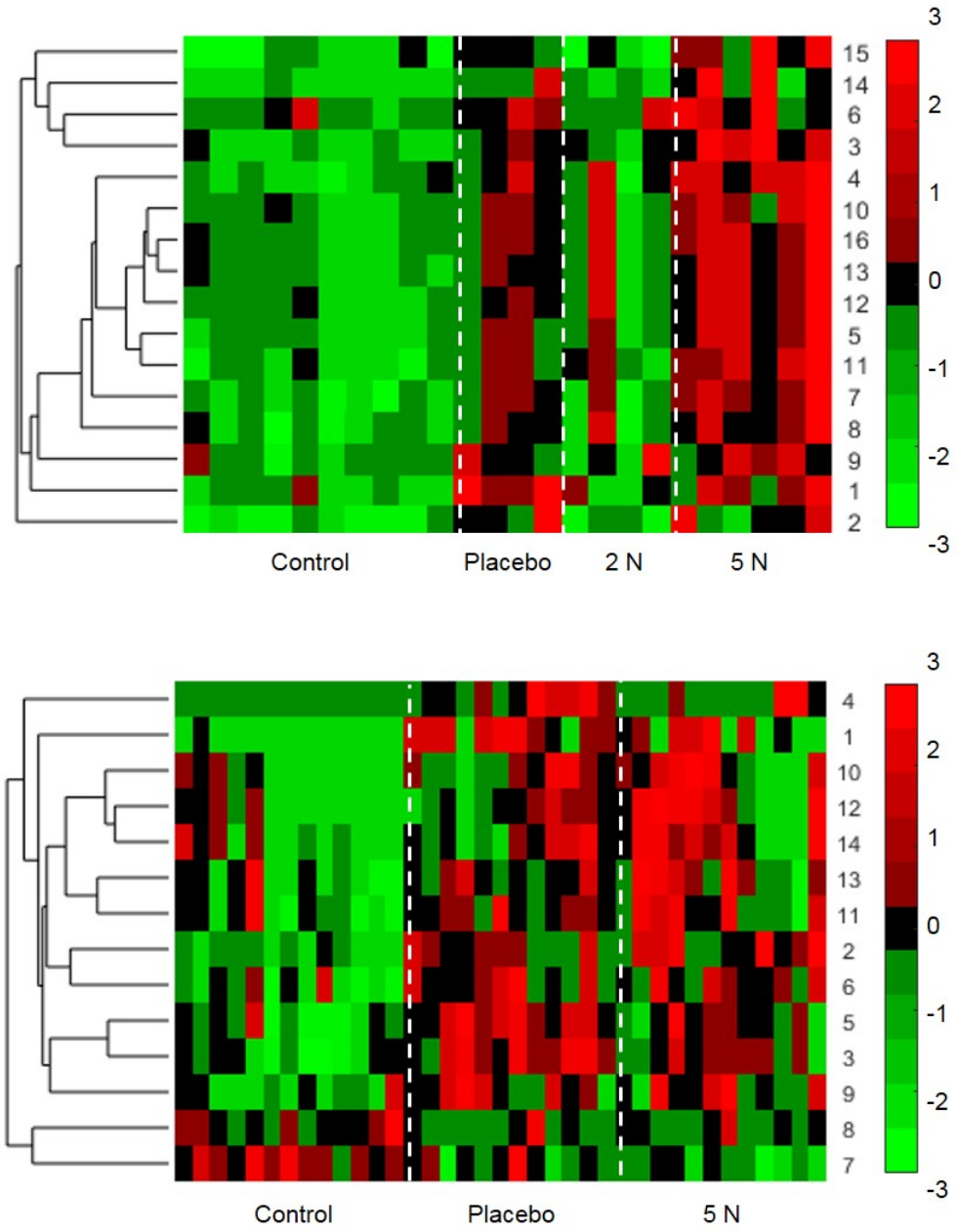

Fig. 3.10.: Hierarchical clustering of statistically significant features (p value<0.05) in placebo and control groups to understand the change in their concentration profiles in urine from (A) C57BL/6 mice with bone tumors (n=4) and control (n=10) (16 features) with 2N Tibia loading (n=4) and 5N Tibia loading (n=6), (B)BALB/c mice with bone tumors (n=12) and control (n=13) (14 features) with 5N Tibia loading (n=12). Samples are across x-axis and VOCs across y-axis.

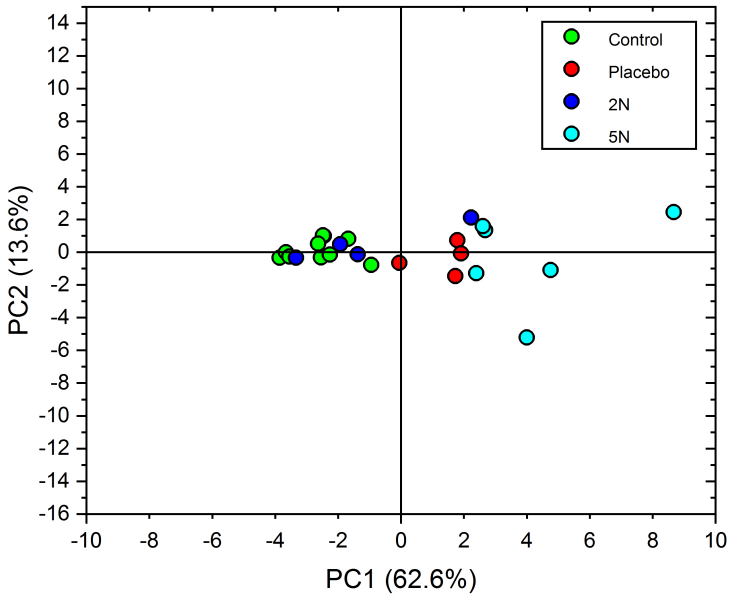

Fig. 3.11.: Principal component analysis of features (p value<0.05) in bone tumor model of C57BL/6 mice (n=4) and controls (n=10) (16 features) to visualize global patterns with the effect of 2N Tibia loading (n=4) and 5N Tibia loading (n=6) treatment.

In C57BL/6 mice, 16 VOCs were statistically significant by Students T-test (p value<0.05). The general distribution of these compounds across four classes can be seen in Figure 3.9.. It is observed that mild compressive strength facilitates healthy bone conditions in VOCs affected by cancer. Moreover, high compressive strength is seen to have a negative effect on homeostasis of bone tissue. These results are confirmed by the hierarchical heatmap comparing placebo and mechanically loaded tumor classes (Figure 3.10.). The overall arrangement of samples on a reduced dimensional space (Figure 3.11.) depicted a trend of low loaded class moving towards control while the high loaded class moves further away from control and placebo class.

In BALB/c mice, 14 VOCs were statistically significant by Students T-test (p value<0.05). Visualization of global patterns of VOCs in these groups indicate the

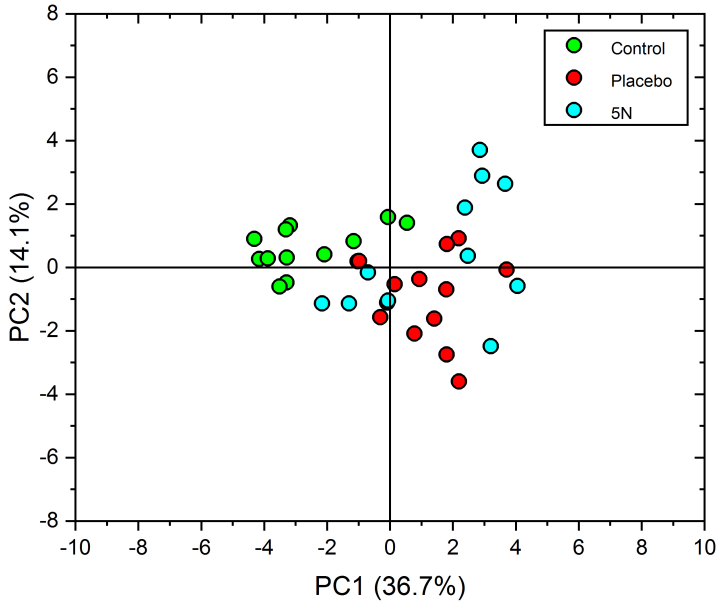

Fig. 3.12.: Principal component analysis of features (p value<0.05) in bone tumor model of BALB/c mice (n=12) and controls (n=13) (14 features) to visualize global patterns with the effect of 5N Tibia loading (n=6) treatment.

ineffectiveness of high compressive strength applied directly at the site of tumor injection (Figure 3.10.). Compounds statistically significant between control and placebo are not positively affected in all mice. Furthermore, principal component analysis of statistically significant compounds demonstrates that while high mechanical loading of the tibia gave adverse responses in C57BL/6 mice, fewer subjects were recognized to look like control mice through their VOC concentrations in the case of BALB/c mice (Figure 3.12.).

Knee loading of mice model of tumor was conducted in C57BL/6 mice giving a matrix of 553 compounds across control, placebo and loading classes. Hierarchical heatmaps of statistically significant compounds in control and placebo class (p value<0.05) showed 14 compounds up-regulated with cancer and moderately restored by knee loading (Figure 3.14.). Similar effect was observed in urinary VOCs down-

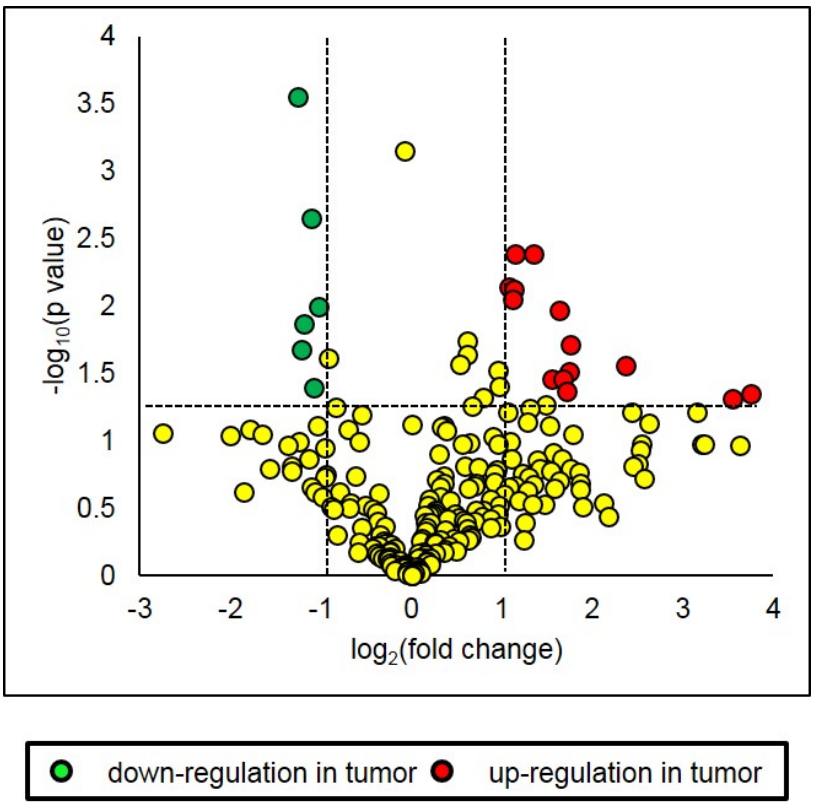

Fig. 3.13.: Volcano plots for overall distribution of 553 urinary VOCs (yellow) in C57BL/6 mice model of bone tumor (n=6) compared to control (n=12). Negative log of p-value from Student's t-test plotted as a function of $\log_2$ fold change. Fold change is the ratio of concentration of a VOC in tumor class to control class. VOCs above the horizontal line are statistically significant (p value$<$0.05) while VOCs with absolute fold change of 1 are located after x=$\pm$1).

regulated with the advent of tumor development. PCA results show 41% variation in sample classes along PC 1 and 16.3% variation along PC 2 (Figure 3.15.). The displacement of knee loading class away from the placebo class point at the prospective success of knee loading in comparison to tibia loading.

Table 3.6.
IUPAC Names of VOCs from Tibia Loading Study in C57BL/6 Mice

VOC ID	IUPAC (Common names)	CAS ID	P-value
1	1-Octen-3-ol	3391-86-4	0.001
2	(2Z)-3,7-dimethylocta-2,6-dien-1-ol	106-25-2	0.044
3	pent-2-en-4-ynyl furan-2-carboxylate	-	0.005
4	2-ethylhexan-1-ol	104-76-7	0.008
5	ethyl 4-ethoxybenzoate	23676-09-7	0.008
6	1-(2,5-dimethylphenyl)ethanone	2142-73-6	0.013
7	[2,3,5,5,8a-Pentamethyl-4a,5,6,7,8,8a-hexahydro-4H -chromene	-	0.013
8	3,5,5-trimethylcyclohex-2-en-1-one	78-59-1	0.013
9	(Z)-non-3-en-1-ol	10340-23-5	0.019
10	undecan-2-one	112-12-9	0.019
11	3-tert-butyl-3,4-dihydro-2H-naphthalen-1-one	42981-74-8	0.038
12	2,4-ditert-butylphenol	96-76-4	0.038
13	(3E,5E)-8,8,9-trimethyldeca-3,5-diene-2,7-dione	-	0.038
14	3-methylbut-2-en-1-ol	556-82-1	0.011
15	[(2S)-6-methyl-2-[(1S)-4-methylcyclohex-3-en-1-yl] hept-5-en-2-ol	515-69-5	0.037
16	2-methoxybenzene-1,4-diol	824-46-4	0.038

Table 3.7.
IUPAC Names of VOCs from Tibia Loading Study in BALB/c Mice

VOC ID	IUPAC (Common names)	CAS ID	P-value
1	5-ethylcyclopentene-1-carboxylic acid	-	0.009
2	1-(2,5-dimethylphenyl)ethanone	2142-73-6	0.00006
3	3-ethyl-3-phenylazetidine-2,4-dione	42282-82-6	0.003
4	methyl 2-methylprop-2-enoate	-	0.0001
5	ethyl 4-ethoxybenzoate	23676-09-7	0.014
6	(E)-4-oxohex-2-enal	2492-43-5	0.010
7	2,4,6-tri(propan-2-yl)phenol	2934-07-8	0.00008
8	(2Z)-3,7-dimethylocta-2,6-dien-1-ol	106-25-2	0.027
9	pent-4-enyl propanoate	-	0.046
10	2-Methoxy-4-methyl-1-pentylbenzene	-	0.014
11	(4R)-1-methyl-4-(6-methylhepta-1,5-dien-2-yl)cyclo hexene	-	0.039
12	1-methoxy-4-(2-methylpropyl)benzene	-	0.027
13	(1S,5S,6R)-4,6-dimethyl-6-(4-methylpent-3-enyl) bicyclo[3.1.1]hept-3-ene	13474-59-4	0.027
14	(4-fluorophenyl)methanol,2-methylpropylether	-	0.027

Table 3.8.
IUPAC Names of VOCs from Knee Loading Study in C57BL/6 Mice

VOC ID	IUPAC (Common names)	CAS ID	P-value
1	ethenyl benzoate	769-78-8	0.0002
2	6-ethoxy-2,2,4-trimethyl-1{H}-quinoline	-	0.0007
3	butan-2-one	78-93-3	0.002
4	(Z)-hexadec-7-ene	35507-6	0.004
5	2,6-di(tert)butyl-4-methylphenol	128-37-0	0.004
6	(E)-4-oxohex-2-enal	2492-43	0.007
7	2-hydroxy-4-propan-2-ylcyclohepta-2,4,6-trien-1-one	-	0.010
8	(3E,6E)-3,7,11-trimethyldodeca-1,3,6,10-tetraene	28973-9	0.010
9	(1S,5S,6S)-2,6-dimethyl-6-(4-methylpent-3-enyl) bicyclo[3.1.1]hept-2-ene	-	0.013
10	4-methyl-1-propan-2-ylcyclohexene	-	0.013
11	hexadecane	544-76-3	0.018
12	(1S)-6,6-dimethyl-2-methylidenebicyclo[3.1.1]heptane	-	0.019
13	3-butan-2-ylcyclohexene	15232-4	0.021
14	hexan-2-one	591-78-6	0.024
15	benzene-1,3-dicarbaldehyde	626-19-7	0.027
16	(Z)-pentadec-6-en-1-ol	-	0.028
17	nonanal	124-19-6	0.030
18	3,7-dimethylocta-1,6-dien-3-ol	78-70-6	0.031
19	(6E)-7,11-dimethyl-3-methylidenedodeca-1,6,10-triene	18794-8	0.034
20	2-methylbut-3-en-2-ol	115-18-4	0.034
21	heptan-2-one	110-43-0	0.040
22	1-hydroxypyridin-4-one	6890-96	0.043

3.6 Terpene/Terpenoid Biosynthesis

Majority of statistically significant VOCs across all studies were identified to belong to the class of terpenes or terpenoids. Pathway analysis of these compounds using KEGG pathway database showed their involvement in cholesterol synthesis axis. Terpenes and steroids are biosynthesized from mevalonate pathway and are precursors of cholesterol and steroid compounds. A plethora of monoterpenoids, sesquiterpenoids, di- and tri-terpenes identified are synthesized from reactions between geranyl pyrophosphate (GPP) and farnesyl pyrophosphate (FPP), that produce building blocks of steroids and cholesterol molecules (Figure 3.16.).

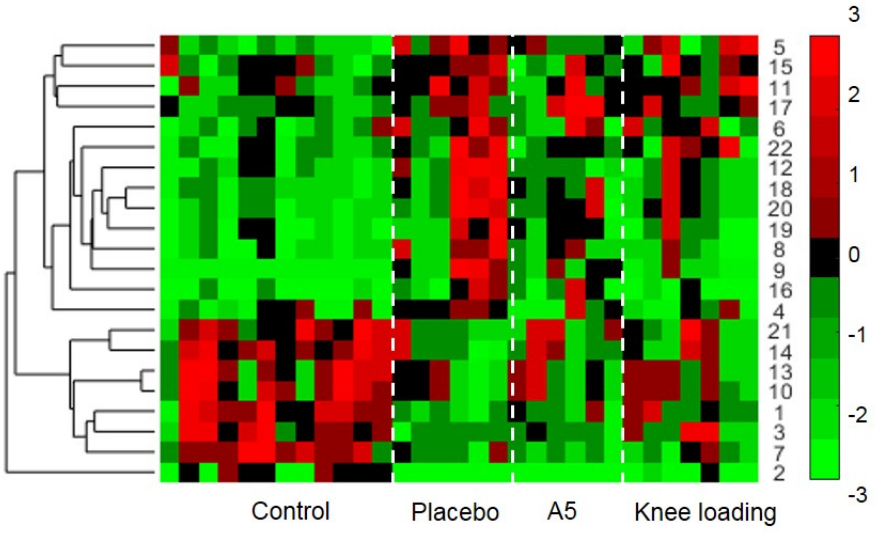

Fig. 3.14.: Hierarchical clustering of statistically significant features (p value<0.05) in placebo and control groups to understand the change in their concentration profiles in urine from C57BL/6 mice with bone tumor (n=6) and control (n=12) (22 features) with A5 treatment (n=6), Knee loading (n=7). Samples are across x-axis and VOCs across y-axis.

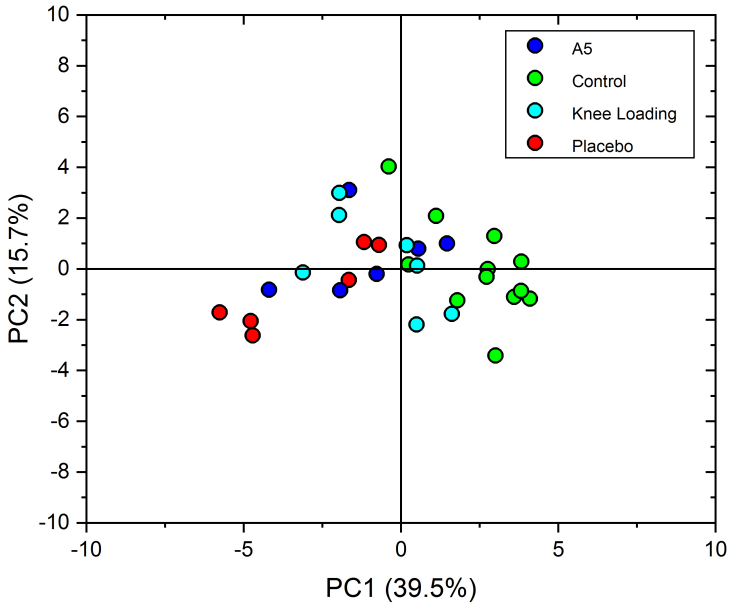

Fig. 3.15.: Principal component analysis of features (p value<0.05) in bone tumor model of C57BL/6 mice (n=6) and controls (n=12) (14 features) to visualize global patterns with the effect of A5 treatment (n=6), Knee loading (n=7) treatment.

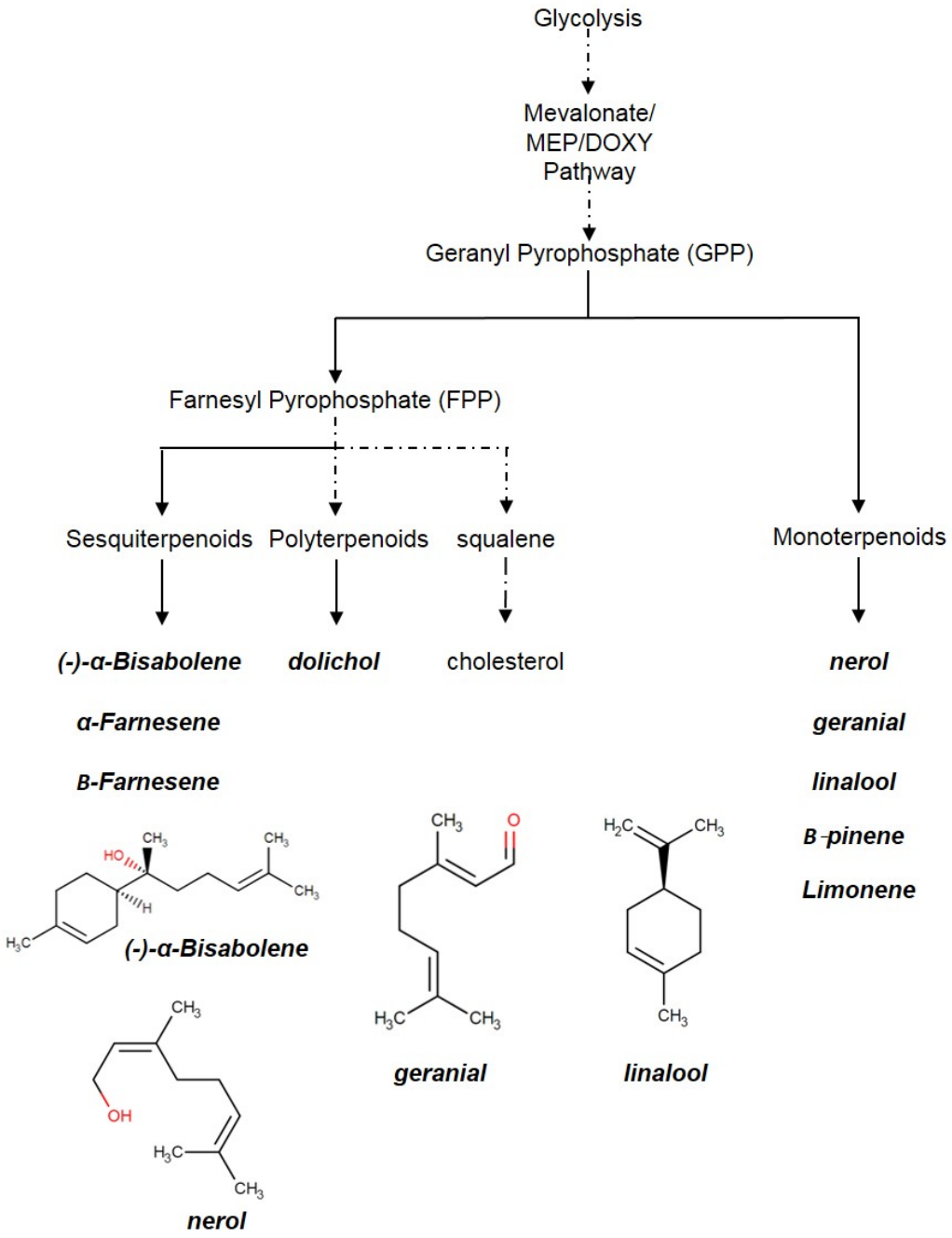

Fig. 3.16.: Metabolic pathway analysis of statistically significant compounds. VOCs identified as terpenes belong to the mevalonate pathway.

4. DISCUSSION

This thesis is based on the study of using urinary VOCs to detect tumors localized in mammary pad or bone of mice by comparing their regulation in healthy mice urine. Results demonstrate the potential of urinary VOCs in distinguishing mice with tumor in either mammary pad or bone from mice without tumor and were validated using statistical procedure of Leave One Out Cross Validation. Metabolic pathway analysis further indicated VOCs from the mevalonate pathway to be significantly affected with tumor growth suggesting its link in cancer pathogenesis. Outcomes of pathway analysis were validated through biological assay of urine cholesterol(results not shown). The second aim of this thesis was to investigate the efficacy of cancer treatments with changes in VOC concentrations. Analyses show effects of both chemical and mechanical treatments on cancer specific VOCs. Treatments with Trifluoperazine, Fluphenazine, Pitavastatin, 2N mechanical force or knee loading showed to have positive effects on tumor bearing mice with their VOC profiles trending towards healthy control class. High mechanical force was ineffective in reinstating levels of VOCs as observed in the urine of healthy controls.

One of the emerging hallmarks of cancer is the deregulation of cellular energetics by manipulating metabolic pathways [83]. Cancer cells thrive on these changes and their control over these become evident with tumor progression [84]. This effect can be observed in panels of VOCs differentially expressed between control and placebo are seen to undergo color transformation in hierarchical heatmaps (Figure 3.3.) corresponding to concentration changes with treatment. The results propose the potential application of VOCs from urine in diagnosing cancer conditions both confined in mammary pad or different location, in this case bone tumor model. They

further demonstrate the capacity of these cancer specific VOCs to predict the success of treatments in restoring transformed metabolism.

Cancer growth involves metabolic alterations with each step of affected pathways considered as an opportunity to hijack metabolic resources [84]. Volcano plots of VOCs are useful in visualizing differences between cancer and healthy conditions (Figure 3.1.,3.6.,3.9.,3.13.) [78, 85]. These plots are instrumental in unveiling the dynamics of tumor interactions with its local tissue environment by the regulation of VOCs and their corresponding pathways. A deeper understanding can be obtained through hierarchical clustering of relevant statistically significant compounds across healthy controls and tumor bearing subjects [86, 87]. These univariate tests aid in a comprehensive interpretation of events observed with the advent of cancer.

The sum of these transformations may, however, not be captured by focusing narrowly on a single VOC as the sole biomarker [81, 88]. Hence, a group of VOCs with the highest ability to distinguish between healthy and diseased condition will have a better predictive value, and may improve biological interpretation [81]. The choice of building a classification model with terpenes and terpenoids, key to the cholesterol pathway, facilitates in greater understanding of the effects of cancer and determining the efficacy of drug treatments. However, there is a tension between (a) building the leanest models possible to reduce the hazards of overfitting the data and (b) describing all relevant results, including the large number of terpenoids/terpenes that may in fact be implicated or analysed to determine treatment efficacy and cancer progression. This balance was achieved by building a predictive model with the fewest compounds possible (models were built by iterative LDA for mammary pad and bone tumor model utilizing four and three VOCs, respectively).

A unique finding of this study is the composition of terpenes and terpenoids in VOCs statistically significant between control and placebo groups across all studies. Terpenoid and steroid biosynthesis is a descending step of the mevalonate pathway and a precursor to cholesterol synthesis [89–91]. There is an intriguing link between terpenoids as markers of cancer and potential treatments for cancer: for example, ter-

penes and terpenoids are known to have inhibitory action against cancer and cholesterol itself has previously been reported to play a role in the development of certain cancers [92]. Biological validation for urine cholesterol levels in healthy controls and tumor bearing mice confirmed these observations through ELISA results (figure not shown).

Chemical drug treatments would be expected to cause a change in mouse urine, including a change in expressed VOCs. As the chemical mode of treatment utilized agents involved in dopaminergic signalling or mevalonate pathway (MVA), it would be expected that dopamine or MVA-related VOCs might be affected by the drug treatment. This study, however, sought to focus on changes caused by treatments on specific VOCs identified as altered by cancer. Moreover, different sets of VOCs are observed in cancers depending on tumor location and interactions with tumor microenvironment [93]. This difference might be linked to cancer cells distinctly manipulating local metabolic pathways to thrive at different sites as seen in mammary pad or bone tumor comparisons with respect to controls. The effect of drug on the tumor, therefore, would be specific to the diseased area. This is evident from the VOC analysis in this experiment, the action of Trifluoperazine in mice model of bone tumor is observed to have a positive effect on bone remodelling than Fluphenazine. Collectively, these two agents have a distinguishable effect on mice with mammary pad tumor model. Alternatively, treatment with Pitavastatin yields moderate positive response in mice in regards to restoration of cancer-specific VOCs.

Treatment with mechanical stimulation of bone in mice model of bone tumor is equivalent to physical exercise as a treatment option. The efficacy of these modalities in recovering from tumor associated variations is demonstrated through hierarchical heatmaps and principal component analysis. The results point out the advantage of loading of the tibia with 2N compressive strength over 5N compressive strength in preventing bone resorption. The overall results although consistent with results from different strain of mouse model, the effect of the treatment in BALB/c mice suggested that each mouse responded differentially to the loading. Treatment with

knee mechanical loading was deemed to be favorable in healing mice as observed through PCA and hierarchical heatmaps.

5. STATISTICAL CONSIDERATIONS

The results of this thesis raise several statistical concerns in selecting VOC biomarkers. First, including compounds present in only 60% of one sample class indicates a loss of useful information which may reflect biological results, but also may be due to technical errors such as presence of a compound in a sample in concentrations below the detection limit. This may weaken confidence in the process of biomarker discovery. Second, while the gas chromatography method used here is sensitive, it has less precision than other analytical methods such as LCMS, suggesting that using a statistical significance level of 0.05 can likely restrict selection of relevant features as probable biomarkers. Both of these filters are ad hoc decisions that can cause biased selection of features. Although it is essential to draw certain threshold limits in analyzing data of cohort untargeted studies, the appropriateness of data analysis procedures used herein needs to be evaluated for identification of reliable biomarkers. Third, small sample size for experiments can considerably affect the outcomes of statistical tests.

Results were evaluated through computational and experimental techniques. Although model validation using Leave One Out Cross Validation suggested a definitive set of biomarkers, building and training models based on initially selected compounds can provide biased outputs. A rigorously verified statistical approach should be employed for identifying true biomarkers. Additional computational simulation or validation techniques have to be utilized for justification of markers. Techniques such as testing on an independent data set, inner cross-validation for feature selection or Monte Carlo simulation should be conducted for further validating compound selection. Experimental evaluation of preliminary metabolic pathway analysis was also confirmed through biological assay of cholesterol urine. It is suggested that there is a probable link of mevalonate pathway and tumor development through proposed VOC

markers. However, detailed computational and biological studies focused on validating identified metabolites have to be conducted in future experiments for improving predictive value of VOCs.

6. CONCLUSIONS

The key finding of this work is that VOC analysis of urine demonstrates a probable method to detect tumor developments at two distinct locations as well as to monitor treatment efficacy. Fifty-four VOCs showed differences in the urine of healthy controls and subjects with tumor in the mammary pad or bone. Metabolic pathway analysis of the identified VOCs indicate a link of mevalonate pathway with tumor development. Statistical and biological procedures evaluated the outcomes of VOC and metabolic pathway analysis. Thus, giving a non-invasive insight into the metabolic alterations caused by cancer. Across five different types of treatment and two different mouse breeds, VOC analyses consistently aligned with histological determinations of efficacy of treatments, suggesting urinary VOCs may one day indicate effectiveness of therapeutic intervention. Analysis of VOC profiles in urine demonstrate chemical and mechanical modes of cancer treatment can significantly reduce cancer effects and restore normal healthy metabolic functions. To conclude, this study provides a non-invasive method for detecting tumors located in mammary pad or bone through urine analysis. It further shows it applicability in determining effects of cancer treatments. VOC analysis of urine is a potential first step in addressing issues of false detection, high operational costs and invasive cancer diagnostic and treatment monitoring techniques.

LIST OF REFERENCES

LIST OF REFERENCES

[1] R. L. Siegel, K. D. Miller, and A. Jemal, "Cancer statistics, 2019," vol. 69, no. 1, pp. 7–34. [Online]. Available: https://doi.org/10.3322/caac.21551

[2] R. Shah, K. Rosso, and S. Nathanson, *Pathogenesis, prevention, diagnosis and treatment of breast cancer*, vol. 5.

[3] J. Hayes, A. Richardson, and C. Frampton, "Population attributable risks for modifiable lifestyle factors and breast cancer in new zealand women," vol. 43, no. 11, pp. 1198–1204. [Online]. Available: https://doi.org/10.1111/imj.12256

[4] A. M. Kabel and F. H. Baali, "Breast cancer: Insights into risk factors, pathogenesis, diagnosis and management," p. 6.

[5] S. Lopez Gordo, J. Blanch Falp, E. Lopez-Gordo, E. Just Roig, J. Encinas Mendez, and J. Seco Calvo, "Influence of ductal carcinoma in situ on the outcome of invasive breast cancer. a prospective cohort study," vol. 63, pp. 98–106. [Online]. Available: https://linkinghub.elsevier.com/retrieve/pii/S1743919119300238

[6] J. Makki, "Diversity of breast carcinoma: Histological subtypes and clinical relevance," vol. 8, pp. 23–31. [Online]. Available: https://www.ncbi.nlm.nih.gov/pmc/articles/PMC4689326/

[7] N. Eliyatkn, E. Yaln, B. Zengel, S. Akta, and E. Vardar, "Molecular classification of breast carcinoma: From traditional, old-fashioned way to a new age, and a new way," vol. 11, no. 2, pp. 59–66. [Online]. Available: https://www.ncbi.nlm.nih.gov/pmc/articles/PMC5351488/

[8] E. A. Rakha, J. S. Reis-Filho, F. Baehner, D. J. Dabbs, T. Decker, V. Eusebi, S. B. Fox, S. Ichihara, J. Jacquemier, S. R. Lakhani, J. Palacios, A. L. Richardson, S. J. Schnitt, F. C. Schmitt, P.-H. Tan, G. M. Tse, S. Badve, and I. O. Ellis, "Breast cancer prognostic classification in the molecular era: the role of histological grade," vol. 12, no. 4, p. 207. [Online]. Available: https://www.ncbi.nlm.nih.gov/pmc/articles/PMC2949637/

[9] O. J. Scully, B.-H. Bay, G. Yip, and Y. Yu, "Breast cancer metastasis," vol. 9, no. 5, pp. 311–320. [Online]. Available: http://cgp.iiarjournals.org/content/9/5/311

[10] M. E. Shaffrey, M. Mut, A. L. Asher, S. H. Burri, A. Chahlavi, S. M. Chang, E. Farace, J. B. Fiveash, S. J. Hentschel, F. F. Lang, M. S. Lopes, J. M. Markert, D. Schiff, V. Siomin, S. B. Tatter, and M. A. Vogelbaum, "Brain metastases," vol. 41, no. 8, pp. 665–741. [Online]. Available: http://www.sciencedirect.com/science/article/pii/S0011384004000504

[11] D. G. Ju, A. Yurter, Z. L. Gokaslan, and D. M. Sciubba, "Diagnosis and surgical management of breast cancer metastatic to the spine," vol. 5, no. 3, pp. 263–271. [Online]. Available: https://www.ncbi.nlm.nih.gov/pmc/articles/PMC4127599/

[12] B. Tayyeb and M. Parvin, "Pathogenesis of breast cancer metastasis to brain: a comprehensive approach to the signaling network," vol. 53, no. 1, pp. 446–454. [Online]. Available: https://app.dimensions.ai/details/publication/pub.1043464024

[13] M. Yousefi, R. Nosrati, A. Salmaninejad, S. Dehghani, A. Shahryari, and A. Saberi, "Organ-specific metastasis of breast cancer: molecular and cellular mechanisms underlying lung metastasis," vol. 41, no. 2, pp. 123–140. [Online]. Available: http://link.springer.com/10.1007/s13402-018-0376-6

[14] I. J. Fidler, "The pathogenesis of cancer metastasis: the 'seed and soil' hypothesis revisited," vol. 3, no. 6, pp. 453–458. [Online]. Available: http://www.nature.com/articles/nrc1098

[15] W. Chen, A. D. Hoffmann, H. Liu, and X. Liu, "Organotropism: new insights into molecular mechanisms of breast cancer metastasis," vol. 2, no. 1. [Online]. Available: http://www.nature.com/articles/s41698-018-0047-0

[16] E. S. McDonald, A. S. Clark, J. Tchou, P. Zhang, and G. M. Freedman, "Clinical diagnosis and management of breast cancer," vol. 57, pp. 9S–16S. [Online]. Available: http://jnm.snmjournals.org/content/57/Supplement_1/9S

[17] L. E. Pace and N. L. Keating, "A systematic assessment of benefits and risks to guide breast cancer screening DecisionsBreast cancer screening DecisionsBreast cancer screening decisions," vol. 311, no. 13, pp. 1327–1335. [Online]. Available: https://dx.doi.org/10.1001/jama.2014.1398

[18] T. B. Bevers, M. Helvie, E. Bonaccio, K. E. Calhoun, M. B. Daly, W. B. Farrar, J. E. Garber, R. Gray, C. C. Greenberg, R. Greenup, N. M. Hansen, R. E. Harris, A. S. Heerdt, T. Helsten, L. Hodgkiss, T. L. Hoyt, J. G. Huff, L. Jacobs, C. D. Lehman, B. Monsees, B. L. Niell, C. C. Parker, M. Pearlman, L. Philpotts, L. B. Shepardson, M. L. Smith, M. Stein, L. Tumyan, C. Williams, M. A. Bergman, and R. Kumar, "Breast cancer screening and diagnosis, version 3.2018, NCCN clinical practice guidelines in oncology," vol. 16, no. 11, pp. 1362–1389. [Online]. Available: http://www.jnccn.org/lookup/doi/10.6004/jnccn.2018.0083

[19] H. C. Thoeny and B. D. Ross, "Predicting and monitoring cancer treatment response with DW-MRI," vol. 32, no. 1, pp. 2–16. [Online]. Available: https://www.ncbi.nlm.nih.gov/pmc/articles/PMC2918419/

[20] S. Radhakrishna, S. Agarwal, P. M. Parikh, K. Kaur, S. Panwar, S. Sharma, A. Dey, K. K. Saxena, M. Chandra, and S. Sud, "Role of magnetic resonance imaging in breast cancer management," vol. 7, no. 2, pp. 69–71. [Online]. Available: https://www.ncbi.nlm.nih.gov/pmc/articles/PMC5909298/

[21] T. K. Egan, "Monitoring patients undergoing cancer therapy," vol. 31, no. 12, pp. 666–671. [Online]. Available: https://dx.doi.org/10.1309/R078-Y40Q-PAJP-1RPP

[22] S.-X. Li, A. Sjolund, L. Harris, and J. B. Sweasy, "DNA repair and personalized breast cancer therapy," vol. 51, no. 8, pp. 897–908. [Online]. Available: https://www.ncbi.nlm.nih.gov/pmc/articles/PMC2962983/

[23] I. A. Umelo, B. Costanza, and V. Castronovo, "Innovative methods for biomarker discovery in the evaluation and development of cancer precision therapies," vol. 37, no. 1, pp. 125–145. [Online]. Available: http://link.springer.com/10.1007/s10555-017-9710-0

[24] L.-H. Gam, "Breast cancer and protein biomarkers," vol. 2, no. 5, pp. 86–91. [Online]. Available: https://www.ncbi.nlm.nih.gov/pmc/articles/PMC3905586/

[25] T. N. Zamay, G. S. Zamay, O. S. Kolovskaya, R. A. Zukov, M. M. Petrova, A. Gargaun, M. V. Berezovski, and A. S. Kichkailo, "Current and prospective protein biomarkers of lung cancer," vol. 9, no. 11. [Online]. Available: https://www.ncbi.nlm.nih.gov/pmc/articles/PMC5704173/

[26] W. Wu and S. Zhao, "Metabolic changes in cancer: beyond the warburg effect," vol. 45, no. 1, pp. 18–26. [Online]. Available: https://academic.oup.com/abbs/article-lookup/doi/10.1093/abbs/gms104

[27] M. I. Nounou, F. ElAmrawy, N. Ahmed, K. Abdelraouf, S. Goda, and H. Syed-Sha-Qhattal, "Breast cancer: Conventional diagnosis and treatment modalities and recent patents and technologies," vol. 9, pp. 17–34. [Online]. Available: https://www.ncbi.nlm.nih.gov/pmc/articles/PMC4589089/

[28] M. Bhardwaj, A. Gies, S. Werner, P. Schrotz-King, and H. Brenner, "Blood-based protein signatures for early detection of colorectal cancer: A systematic review," vol. 8, no. 11, p. e128. [Online]. Available: https://www.ncbi.nlm.nih.gov/pmc/articles/PMC5717517/

[29] A. G. Waks and E. P. Winer, "Breast cancer treatment: A review," vol. 321, no. 3, pp. 288–300. [Online]. Available: https://jamanetwork.com/journals/jama/fullarticle/2721183

[30] G. Bonadonna, E. Brusamolino, P. Valagussa, A. Rossi, L. Brugnatelli, C. Brambilla, M. De Lena, G. Tancini, E. Bajetta, R. Musumeci, and U. Veronesi, "Combination chemotherapy as an adjuvant treatment in operable breast cancer," vol. 294, no. 8, pp. 405–410. [Online]. Available: https://doi.org/10.1056/NEJM197602192940801

[31] C. K. Osborne, "Tamoxifen in the treatment of breast cancer," vol. 339, no. 22, pp. 1609–1618. [Online]. Available: https://doi.org/10.1056/NEJM199811263392207

[32] D. Mauri, J. P. A. Ioannidis, and N. Pavlidis, "Neoadjuvant versus adjuvant systemic treatment in breast cancer: A meta-analysis," vol. 97, no. 3, pp. 188–194. [Online]. Available: https://doi.org/10.1093/jnci/dji021

[33] N. Masuda, S.-J. Lee, S. Ohtani, Y.-H. Im, E.-S. Lee, I. Yokota, K. Kuroi, S.-A. Im, B.-W. Park, S.-B. Kim, Y. Yanagita, S. Ohno, S. Takao, K. Aogi, H. Iwata, J. Jeong, A. Kim, K.-H. Park, H. Sasano, Y. Ohashi, and M. Toi, "Adjuvant capecitabine for breast cancer after preoperative chemotherapy," vol. 376, no. 22, pp. 2147–2159. [Online]. Available: https://doi.org/10.1056/NEJMoa1612645

[34] C.-T. Yeh, A. T. H. Wu, P. M.-H. Chang, K.-Y. Chen, C.-N. Yang, S.-C. Yang, C.-C. Ho, C.-C. Chen, Y.-L. Kuo, P.-Y. Lee, Y.-W. Liu, C.-C. Yen, M. Hsiao, P.-J. Lu, J.-M. Lai, L.-S. Wang, C.-H. Wu, J.-F. Chiou, P.-C. Yang, and C.-Y. F. Huang, "Trifluoperazine, an antipsychotic agent, inhibits cancer stem cell growth and overcomes drug resistance of lung cancer," vol. 186, no. 11, pp. 1180–1188. [Online]. Available: https://doi.org/10.1164/rccm.201207-1180OC

[35] R. Y. A. Mukhtar, J. Reid, and J. P. D. Reckless, "Pitavastatin," vol. 59, no. 2, pp. 239–252. [Online]. Available: https://onlinelibrary.wiley.com/doi/abs/10.1111/j.1742-1241.2005.00461.x

[36] Diagnostic & monitoring tests | cancer testing | UNM cancer center. [Online]. Available: http://cancer.unm.edu/cancer/cancer-info/testing-overview/diagnostics-monitoring-tests/

[37] S. J. Dawson, D. W. Tsui, M. Murtaza, H. Biggs, O. M. Rueda, S. F. Chin, M. J. Dunning, D. Gale, T. Forshew, B. Mahler-Araujo, S. Rajan, S. Humphray, J. Becq, D. Halsall, M. Wallis, D. Bentley, C. Caldas, and N. Rosenfeld, "Analysis of circulating tumor DNA to monitor metastatic breast cancer," vol. 368. [Online]. Available: https://doi.org/10.1056/NEJMoa1213261

[38] P. Razavi, B. T. Li, C. Hou, R. Shen, O. Venn, R. S. Lim, E. Hubbell, I. De Bruijn, Q. Liu, R. Vijaya Satya, H. Xu, L. Shen, A. Sehnert, T. Maddala, M. F. Berger, A. Aravanis, J. S. Reis-Filho, M. Lee, D. B. Solit, and J. Baselga, "Cell-free DNA (cfDNA) mutations from clonal hematopoiesis: Implications for interpretation of liquid biopsy tests." vol. 35, no. 15, pp. 11 526–11 526. [Online]. Available: https://doi.org/10.1200/JCO.2017.35.15_suppl.11526

[39] Z. Feng, Y. Xia, T. Gao, F. Xu, Q. Lei, C. Peng, Y. Yang, Q. Xue, X. Hu, Q. Wang, R. Wang, Z. Ran, Z. Zeng, N. Yang, Z. Xie, and L. Yu, "The antipsychotic agent trifluoperazine hydrochloride suppresses triple-negative breast cancer tumor growth and brain metastasis by inducing g0/g1 arrest and apoptosis," vol. 9, no. 10, p. 1006. [Online]. Available: https://doi.org/10.1038/s41419-018-1046-3

[40] R. Hilf, C. Bell, H. Goldenberg, and I. Michel, "Effect of fluphenazine HC1 on r3230ac mammary carcinoma and mammary glands of the rat," vol. 31, p. 8.

[41] B. A. Abdelmaksoud, "Role of statins in breast cancer management: Current issues and future directions," vol. 3, no. 5. [Online]. Available: https://juniperpublishers.com/ctoij/CTOIJ.MS.ID.555624.php

[42] A. Gbel, A. J. Browne, S. Thiele, M. Rauner, L. C. Hofbauer, and T. D. Rachner, "Potentiated suppression of dickkopf-1 in breast cancer by combined administration of the mevalonate pathway inhibitors zoledronic acid and statins," vol. 154, no. 3, pp. 623–631. [Online]. Available: http://link.springer.com/10.1007/s10549-015-3624-8

[43] N. Berndt, A. D. Hamilton, and S. M. Sebti, "Targeting protein prenylation for cancer therapy," vol. 11, no. 11, pp. 775–791. [Online]. Available: https://www.ncbi.nlm.nih.gov/pmc/articles/PMC4037130/

[44] D. Hanahan and R. Weinberg, "Hallmarks of cancer: The next generation," vol. 144, no. 5, pp. 646–674. [Online]. Available: https://linkinghub.elsevier.com/retrieve/pii/S0092867411001279

[45] A. Marusyk and K. Polyak, "Tumor heterogeneity: causes and consequences," vol. 2010.

[46] J. D. Potter, J. R. Cerhan, T. A. Sellers, P. G. McGovern, C. Drinkard, L. R. Kushi, and A. R. Folsom, "Progesterone and estrogen receptors and mammary neoplasia in the iowa women's health study: how many kinds of breast cancer are there?" vol. 4, no. 4, p. 319. [Online]. Available: http://cebp.aacrjournals.org/content/4/4/319.abstract

[47] L. G. Martelotto, C. K. Ng, S. Piscuoglio, B. Weigelt, and J. S. Reis-Filho, "Breast cancer intra-tumor heterogeneity," vol. 16, no. 3, p. 210. [Online]. Available: https://doi.org/10.1186/bcr3658

[48] "An omics perspective on cancer research," OCLC: ocn501392172.

[49] P. Kalita-de Croft, F. Al-Ejeh, A. E. McCart Reed, J. M. Saunus, and S. R. Lakhani, "omics approaches in breast cancer research and clinical practice," vol. 23, no. 6. [Online]. Available: https://journals.lww.com/anatomicpathology/Fulltext/2016/11000/_Omics_Approaches_in_Breast_Cancer_Research_and.2.aspx

[50] W. B. Coleman and G. J. Tsongalis, *Molecular Pathology: The Molecular Basis of Human Disease*. Academic Press, google-Books-ID: BfVeBwAAQBAJ.

[51] A. S. Coates, E. P. Winer, A. Goldhirsch, R. D. Gelber, M. Gnant, M. Piccart-Gebhart, B. Thrlimann, and H.-J. Senn, "Tailoring therapiesimproving the management of early breast cancer: St gallen international expert consensus on the primary therapy of early breast cancer 2015," vol. 26, no. 8, pp. 1533–1546. [Online]. Available: https://www.ncbi.nlm.nih.gov/pmc/articles/PMC4511219/

[52] M. Monteiro, M. Carvalho, M. de Lourdes Bastos, and P. Guedes de Pinho, "Potentiality of volatiles to discriminate patients with cancer by using chemometric tools." pp. 167–184.

[53] C. Xuan, J. M. Shamonki, A. Chung, M. L. DiNome, M. Chung, P. A. Sieling, and D. J. Lee, "Microbial dysbiosis is associated with human breast cancer," vol. 9, no. 1, p. e83744. [Online]. Available: https://doi.org/10.1371/journal.pone.0083744

[54] A. K. Greenberg and M. S. Lee, "Biomarkers for lung cancer: clinical uses," vol. 13, no. 4. [Online]. Available: https://journals.lww.com/co-pulmonarymedicine/Fulltext/2007/07000/Biomarkers_for_lung_cancer__clinical_uses.3.aspx

[55] L. Lavra, A. Catini, A. Ulivieri, R. Capuano, L. Baghernajad Salehi, S. Sciacchitano, A. Bartolazzi, S. Nardis, R. Paolesse, E. Martinelli, and C. Di Natale, "Investigation of VOCs associated with different characteristics of breast cancer cells," vol. 5, p. 13246. [Online]. Available: https://doi.org/10.1038/srep13246

[56] C. L. Silva, M. Passos, and J. S. Cmara, "Solid phase microextraction, mass spectrometry and metabolomic approaches for detection of potential urinary cancer biomarkersa powerful strategy for breast cancer diagnosis," vol. 89, pp. 360–368. [Online]. Available: https://linkinghub.elsevier.com/retrieve/pii/S003991401101109X

[57] Y. Hanai, K. Shimono, H. Oka, Y. Baba, K. Yamazaki, and G. K. Beauchamp, "Analysis of volatile organic compounds released from human lung cancer cells and from the urine of tumor-bearing mice," vol. 12, no. 1, p. 7. [Online]. Available: https://doi.org/10.1186/1475-2867-12-7

[58] A. P. Siegel, A. Daneshkhah, D. S. Hardin, S. Shrestha, K. Varahramyan, and M. Agarwal, "Analyzing breath samples of hypoglycemic events in type 1 diabetes patients: towards developing an alternative to diabetes alert dogs," vol. 11, no. 2, p. 026007. [Online]. Available: http://stacks.iop.org/1752-7163/11/i=2/a=026007?key=crossref.5d01147056cfee272470f7fc7300b86c

[59] M. Phillips, "Method for the collection and assay of volatile organic compounds in breath," vol. 247, no. 2, pp. 272–278. [Online]. Available: http://linkinghub.elsevier.com/retrieve/pii/S0003269797920698

[60] M. Phillips, J. Herrera, S. Krishnan, M. Zain, J. Greenberg, and R. N. Cataneo, "Variation in volatile organic compounds in the breath of normal humans," vol. 729, no. 1, pp. 75–88. [Online]. Available: http://www.sciencedirect.com/science/article/pii/S0378434799001279

[61] M. Mandy, F. Cornelia, L. Malgorzata, S. Oliver, S. Achim, and S. Dorothee, "Volatile organic compounds (VOCs) in exhaled breath of patients with breast cancer in a clinical setting," p. 7.

[62] G. Peng, M. Hakim, Y. Y. Broza, S. Billan, R. Abdah-Bortnyak, A. Kuten, U. Tisch, and H. Haick, "Detection of lung, breast, colorectal and prostate cancers from exhaled breath using a single array of nanosensors," vol. 103, no. 4, pp. 542–551. [Online]. Available: http://www.nature.com/articles/6605810

[63] M. Phillips, R. N. Cataneo, C. Saunders, P. Hope, P. Schmitt, and J. Wai, "Volatile biomarkers in the breath of women with breast cancer," vol. 4, no. 2, p. 026003. [Online]. Available: http://stacks.iop.org/1752-7163/4/i=2/a=026003?key=crossref.848f7b548bd5b6c15f05fd62240358e6

[64] M. Phillips, R. N. Cataneo, B. A. Ditkoff, P. Fisher, J. Greenberg, R. Gunawardena, C. S. Kwon, F. Rahbari-Oskoui, and C. Wong, "Volatile markers of breast cancer in the breath," vol. 9, no. 3, pp. 184–191. [Online]. Available: https://doi.org/10.1046/j.1524-4741.2003.09309.x

[65] S. Esfahani, A. Wicaksono, E. Mozdiak, R. P. Arasaradnam, and J. A. Covington, "Non-invasive diagnosis of diabetes by volatile organic compounds in urine using FAIMS and fox4000 electronic nose," vol. 8, no. 4. [Online]. Available: https://www.ncbi.nlm.nih.gov/pmc/articles/PMC6316010/

[66] T. Khalid, R. Aggio, P. White, B. De Lacy Costello, R. Persad, H. Al-Kateb, P. Jones, C. S. Probert, and N. Ratcliffe, "Urinary volatile organic compounds for the detection of prostate cancer," vol. 10, no. 11. [Online]. Available: https://www.ncbi.nlm.nih.gov/pmc/articles/PMC4657998/

[67] T. H. More, S. RoyChoudhury, J. Christie, K. Taunk, A. Mane, M. K. Santra, K. Chaudhury, and S. Rapole, "Metabolomic alterations in invasive ductal carcinoma of breast: A comprehensive metabolomic study using tissue and serum samples," vol. 9, no. 2, pp. 2678–2696. [Online]. Available: https://www.ncbi.nlm.nih.gov/pmc/articles/PMC5788669/

[68] C. D. Hart, L. Tenori, C. Luchinat, and A. Di Leo, "Metabolomics in breast cancer: Current status and perspectives," in *Novel Biomarkers in the Continuum of Breast Cancer*, ser. Advances in Experimental Medicine and Biology, V. Stearns, Ed. Springer International Publishing, pp. 217–234. [Online]. Available: https://doi.org/10.1007/978-3-319-22909-6_9

[69] J. Budczies and C. Denkert, "Tissue-based metabolomics to analyze the breast cancer metabolome," in *Metabolism in Cancer*, ser. Recent Results in Cancer Research, T. Cramer and C. A. Schmitt, Eds. Springer International Publishing, pp. 157–175. [Online]. Available: https://doi.org/10.1007/978-3-319-42118-6_7

[70] Y. Fan, X. Zhou, T.-S. Xia, Z. Chen, J. Li, Q. Liu, R. N. Alolga, Y. Chen, M.-D. Lai, P. Li, W. Zhu, and L.-W. Qi, "Human plasma metabolomics for identifying differential metabolites and predicting molecular subtypes of breast cancer," vol. 7, no. 9, pp. 9925–9938. [Online]. Available: http://www.oncotarget.com/index.php?journal=oncotarget&page=article&op=view&path[]=7155&path[]=20380

[71] G. Echeverry, G. L. Hortin, and A. J. Rai, "Introduction to urinalysis: Historical perspectives and clinical application," in *The Urinary Proteome: Methods and Protocols*, ser. Methods in Molecular Biology, A. J. Rai, Ed. Humana Press, pp. 1–12. [Online]. Available: https://doi.org/10.1007/978-1-60761-711-2_1

[72] M. Li, "Urine reflection of changes in blood," in *Urine Proteomics in Kidney Disease Biomarker Discovery*, ser. Advances in Experimental Medicine and Biology, Y. Gao, Ed. Springer Netherlands, pp. 13–19. [Online]. Available: https://doi.org/10.1007/978-94-017-9523-4_2

[73] S. Liu, Y. Fan, A. Chen, A. Jalali, K. Minami, K. Ogawa, H. Nakshatri, B.-Y. Li, and H. Yokota, "Osteocyte-driven downregulation of snail restrains effects of drd2 inhibitors on mammary tumor cells," vol. 78, no. 14, p. 3865. [Online]. Available: http://cancerres.aacrjournals.org/content/78/14/3865.abstract

[74] B. Li, J. Tang, Q. Yang, S. Li, X. Cui, Y. Li, Y. Chen, W. Xue, X. Li, and F. Zhu, "NOREVA: normalization and evaluation of MS-based metabolomics data," vol. 45, pp. W162–W170. [Online]. Available: https://academic.oup.com/nar/article-lookup/doi/10.1093/nar/gkx449

[75] A. Ghasemi and S. Zahediasl, "Normality tests for statistical analysis: A guide for non-statisticians," vol. 10, no. 2, pp. 486–489. [Online]. Available: https://www.ncbi.nlm.nih.gov/pmc/articles/PMC3693611/

[76] H.-Y. Kim, "Statistical notes for clinical researchers: assessing normal distribution (2) using skewness and kurtosis," vol. 38, no. 1, pp. 52–54. [Online]. Available: https://www.ncbi.nlm.nih.gov/pmc/articles/PMC3591587/

[77] E. Saccenti, H. C. J. Hoefsloot, A. K. Smilde, J. A. Westerhuis, and M. M. W. B. Hendriks, "Reflections on univariate and multivariate analysis of metabolomics data," vol. 10, no. 3, pp. 361–374. [Online]. Available: https://doi.org/10.1007/s11306-013-0598-6

[78] N. Kumar, M. A. Hoque, and M. Sugimoto, "Robust volcano plot: identification of differential metabolites in the presence of outliers," vol. 19, no. 1, p. 128. [Online]. Available: https://doi.org/10.1186/s12859-018-2117-2

[79] F. Murtagh and P. Contreras, "Algorithms for hierarchical clustering: an overview, II," vol. 7, no. 6, p. e1219. [Online]. Available: https://doi.org/10.1002/widm.1219

[80] Y. Liu, M. P. Vincenti, and H. Yokota, "Principal component analysis for predicting transcription-factor binding motifs from array-derived data," vol. 6, no. 1, p. 276. [Online]. Available: https://doi.org/10.1186/1471-2105-6-276

[81] J. Xia, D. I. Broadhurst, M. Wilson, and D. S. Wishart, "Translational biomarker discovery in clinical metabolomics: an introductory tutorial," vol. 9, no. 2, pp. 280–299. [Online]. Available: https://doi.org/10.1007/s11306-012-0482-9

[82] L. Cella, V. DAvino, R. Liuzzi, M. Conson, F. Doria, A. Faiella, F. Loffredo, M. Salvatore, and R. Pacelli, "Multivariate normal tissue complication probability modeling of gastrointestinal toxicity after external beam radiotherapy for localized prostate cancer," vol. 8, p. 221. [Online]. Available: https://www.ncbi.nlm.nih.gov/pmc/articles/PMC3852304/

[83] D. Hanahan and R. A. Weinberg, "Hallmarks of cancer: the next generation," vol. 144. [Online]. Available: https://doi.org/10.1016/j.cell.2011.02.013

[84] S.-Y. Kim, "Cancer energy metabolism: Shutting power off cancer factory," vol. 26, no. 1, pp. 39–44. [Online]. Available: https://www.ncbi.nlm.nih.gov/pmc/articles/PMC5746036/

[85] M. Hur, A. A. Campbell, M. Almeida-de Macedo, L. Li, N. Ransom, A. Jose, M. Crispin, B. J. Nikolau, and E. S. Wurtele, "A global approach to analysis and interpretation of metabolic data for plant natural product discovery," vol. 30, no. 4, pp. 565–583. [Online]. Available: https://www.ncbi.nlm.nih.gov/pmc/articles/PMC3629923/

[86] P. H. Benton, J. Ivanisevic, D. Rinehart, A. Epstein, M. E. Kurczy, M. D. Boska, H. E. Gendelman, and G. Siuzdak, "An interactive cluster heat map to visualize and explore multidimensional metabolomic data," vol. 11, no. 4, pp. 1029–1034. [Online]. Available: https://www.ncbi.nlm.nih.gov/pmc/articles/PMC4505375/

[87] J.-Y. Moon, H.-J. Jung, M. H. Moon, B. C. Chung, and M. H. Choi, "Heat-map visualization of gas chromatography-mass spectrometry based quantitative signatures on steroid metabolism," vol. 20, no. 9, pp. 1626–1637. [Online]. Available: http://www.sciencedirect.com/science/article/pii/S1044030509003390

[88] B. Xi, H. Gu, H. Baniasadi, and D. Raftery, "Statistical analysis and modeling of mass spectrometry-based metabolomics data," vol. 1198, pp. 333–353. [Online]. Available: https://www.ncbi.nlm.nih.gov/pmc/articles/PMC4319703/

[89] KEGG PATHWAY: Terpenoid backbone biosynthesis - reference pathway. [Online]. Available: https://www.genome.jp/kegg-bin/show_pathway?map00900

[90] KEGG PATHWAY: Monoterpenoid biosynthesis - reference pathway. [Online]. Available: https://www.genome.jp/kegg-bin/show_pathway?map00902

[91] KEGG PATHWAY: Sesquiterpenoid and triterpenoid biosynthesis - reference pathway. [Online]. Available: https://www.genome.jp/kegg-bin/show_pathway?map=map00909&show_description=show

[92] G. Llaverias, C. Danilo, I. Mercier, K. Daumer, F. Capozza, T. M. Williams, F. Sotgia, M. P. Lisanti, and P. G. Frank, "Role of cholesterol in the development and progression of breast cancer," vol. 178, no. 1, pp. 402–412. [Online]. Available: https://www.ncbi.nlm.nih.gov/pmc/articles/PMC3069824/

[93] M. Woollam, M. Teli, P. Angarita-Rivera, S. Liu, A. P. Siegel, H. Yokota, and M. Agarwal, "Detection of volatile organic compounds (VOCs) in urine via gas chromatography-mass spectrometry QTOF to differentiate between localized and metastatic models of breast cancer," vol. 9, no. 1, p. 2526. [Online]. Available: https://doi.org/10.1038/s41598-019-38920-0